

**PURDUE UNIVERSITY
GRADUATE SCHOOL
Thesis/Dissertation Acceptance**

This is to certify that the thesis/dissertation prepared

By Seung Joon Kim

Entitled
Effects of Collagen Gel Stiffness on Cdc42 Activities of Endothelial Colony Forming Cells during
Early Vacuole Formation

For the degree of Master of Science in Biomedical Engineering

Is approved by the final examining committee:

Sungsoo Na

Chair

Dong Xie

Jiliang Li

To the best of my knowledge and as understood by the student in the *Research Integrity and Copyright Disclaimer (Graduate School Form 20)*, this thesis/dissertation adheres to the provisions of Purdue University's "Policy on Integrity in Research" and the use of copyrighted material.

Approved by Major Professor(s): Sungsoo Na

Approved by: John H. Schild

Head of the Graduate Program

05/07/2012

Date

**PURDUE UNIVERSITY
GRADUATE SCHOOL**

Research Integrity and Copyright Disclaimer

Title of Thesis/Dissertation:

Effects of Collagen Gel Stiffness on Cdc42 Activities of Endothelial Colony Forming Cells during Early Vacuole Formation

For the degree of Master of Science in Biomedical Engineering

I certify that in the preparation of this thesis, I have observed the provisions of *Purdue University Executive Memorandum No. C-22*, September 6, 1991, *Policy on Integrity in Research*.*

Further, I certify that this work is free of plagiarism and all materials appearing in this thesis/dissertation have been properly quoted and attributed.

I certify that all copyrighted material incorporated into this thesis/dissertation is in compliance with the United States' copyright law and that I have received written permission from the copyright owners for my use of their work, which is beyond the scope of the law. I agree to indemnify and save harmless Purdue University from any and all claims that may be asserted or that may arise from any copyright violation.

Seung Joon Kim

Printed Name and Signature of Candidate

05/15/2012

Date (month/day/year)

*Located at http://www.purdue.edu/policies/pages/teach_res_outreach/c_22.html

EFFECTS OF COLLAGEN GEL STIFFNESS ON CDC42 ACTIVITIES OF
ENDOTHELIAL COLONY FORMING CELLS DURING EARLY VACUOLE
FORMATION

A Thesis
Submitted to the Faculty
of
Purdue University
by
Seung Joon Kim

In Partial Fulfillment of the
Requirements for the Degree
of
Master of Science in Biomedical Engineering

August 2012
Purdue University
Indianapolis, Indiana

ACKNOWLEDGEMENTS

Firstly I would like to express my greatest gratitude to my advisor, Dr. Sungsoo Na for his mentoring and guidance throughout my Master's degree. His abundance of knowledge and expertise has inspired me to learn research procedures. I would like to thank my thesis committees, Dr. Dong Xie and Dr. Jiliang Li for their encouragement and feedback in my thesis defense. I would also like to thank Dr. Mervin Yoder for providing cells and Dr. Sherry Habrin-Voytik for providing collagen.

I am also very thankful to Dr. Doo-Hun Kim, Dr. Kong Hwan Kim and Dr. Hyun Chul Yoon for their support while I was in an undergraduate degree. I would also like to thank Qiaoqiao Wan and Eun Hye Cho for their support in the laboratory. Appreciation is given to Valerie Lim Diemer for assistance that she has provided in preparing thesis. I would like to thank Paul Crister for his discussion with research and Hee Jin Hwang and So Hyun Park for their sharing research experience. I am thankful to elder Noh and Pastor Cho for taking care of me while staying in Indianapolis.

Lastly, I offer my best regards to my parents and friends for their endless support during the completion of this dissertation.

TABLE OF CONTENTS

	Page
LIST OF TABLES	v
LIST OF FIGURES	vi
ABSTRACT	vi
1. INTRODUCTION	1
1.1 Endothelial Progenitor Cells in Vasculogenesis	2
1.2 Matrices for in vitro Vasculogenesis.....	4
1.2.1 2D Scaffolds.....	5
1.2.2 3D Scaffolds.....	6
1.3 Matrix Stiffness and in vitro Vasculogenesis.....	7
1.3.1 Mechanical Properties of a 2D Gel in Vasculogenesis	7
1.3.2 Mechanical Properties of a 3D Gel in Vasculogenesis	8
1.4 Molecular Mechanisms of in vitro Vasculogenesis	10
1.4.1 Integrins in Vasculogenesis.....	11
1.4.2 Rho GTPases in Vasculogenesis	11
1.4.3 The Role of MT1-MMP in Vasculogenesis	14
1.4.4 Recent Findings of Molecular Pathways in Vasculogenesis.....	15
1.5 FRET Microscopy	16
1.5.1 Rho GTPases Biosensor based on FRET.....	16
1.5.2 Optical Setup of Microscopy	17
1.6 Thesis Objectives.....	18
2. METHODS	20
2.1 Cell Maintenance	20
2.2 DNA Plasmids and Transfection.....	20
2.3 Fabrication of Collagen Gel.....	21
2.4 In vitro Early Vacuole Formation Model.....	22
2.5 FRET Microscopy.....	23
2.6 Image Processing	24
2.7 Data Analysis	25
2.8 Statistical Analysis.....	25

	Page
3. RESULTS	26
3.1 Time-lapse Imaging of ECFC Vacuole Formation in 3D Collagen Matrices	26
3.2 Cdc42 is Activated at Vacuole Sites	27
3.3 Cdc42 Activity is Increased in Soft Matrices during Early Vacuole Formation	28
3.4 Vacuole were Formed Earlier in Soft Matrices than in Rigid Matrices	30
3.5 Vacuole Area is not Dependent on Matrix Stiffness	31
3.6 Early Vacuole Formation is Mediated in Part by Cdc42	32
4. DISCUSSION	34
LIST OF REFERENCES	38

LIST OF TABLES

Table	Page
Table 1.1 Mechanical properties and vasculogenesis	9
Table 2.1 Summary of shear storage modulus of collagen matrices by the collagen polymerization composition	21

LIST OF FIGURES

Figure	Page
Figure 1.1 Morphogenetic steps of the remodeling blood vessels.....	2
Figure 1.2 Schematic diagram of EPCs homing and incorporation into tissue	3
Figure 1.3 ECs in 2D culture form cord-like structure whereas ECs in 3D culture generate lumens	6
Figure 1.4 Model of vascular lumen formation and signal pathway.....	10
Figure 1.5 Signal pathway of vacuole and lumen formation	13
Figure 1.6 Structure of FRET-based Cdc42 biosensor.....	17
Figure 1.7 The outline of optical setup of the FRET microscope system.....	18
Figure 2.1 The relationship between shear storage modulus and collagen quantity.....	21
Figure 2.2 Schematic diagram of experimental procedure.....	22
Figure 2.3 Flow chart of the preparation RS II.....	23
Figure 2.4 The procedure of FRET ratio image generation by using the imageJ software	24
Figure 3.1 Representative images of vacuole forming cells. (A) DIC, (B) YFP, (C) YFP/CFP emission ratio images, (D) 3D-projection image (E) z-stack orthogonal images. White arrowheads indicate vacuole. Scale bar = 10 μm	26
Figure 3.2 Plot profile of Cdc42 activity along the line on the cell body. The graph shows that Cdc42 activation is highly activated in both (A) soft (150 Pa) matrices and (B) rigid (1 kPa) matrices. Scale bar = 10 μm	28

Figure	Page
Figure 3.3	
Time-lapse images of ECFCs during early vacuole formation. (A) Vacuole is formed at 1h after cytokines treatment in soft (150 Pa) matrices and Cdc42 is highly activated near vacuole area. (B) Vacuole is formed at 2 h after cytokines treatment in rigid (1 kPa) matrices. Right-bottom enlarged image shows high Cdc42 activation near vacuole area. Color bars represent emission ratio of YFP/CFP of the biosensor, an index of Cdc42 activation. Images of YFP/CFP are scaled according to the corresponding color bars. The white boxes are cropped and enlarged for better visualization. White and black arrowheads indicate vacuoles in all figures. Scale bars = 10 μm	29
Figure 3.4	
Time courses of Cdc42 activation during early vacuole formation. Cdc42 is highly activated at 3 h in soft (150 Pa) matrices during early vacuole formation. Time courses of YFP/CFP emission ratio are averaged over the whole cells and normalized to time point 0 h. Data represent mean \pm SEM.....	30
Figure 3.5	
The kinetics of early vacuole formation. Vacuoles formed earlier in soft matrices than rigid matrices	30
Figure 3.6	
The effect of matrix stiffness on vacuole area. Vacuole area is not dependent on matrix stiffness. Soft matrices (n = 46, n = cells) and rigid matrices (n = 49) do not show a significant difference. Data represent mean \pm SEM.....	31
Figure 3.7	
Expression of GFP-actin by mutants transfected ECFCs. (A) Cdc42-L61 promoted vacuole formation while transfection with (B) Cdc42-N17 inhibited vacuole formation. Scale bar = 10 μm	32
Figure 3.8	
The effect of Cdc42 on vacuole formation. Early vacuole formation is mediated in part by Cdc42. (A) Treatment of Cdc42-L61 (n = 20, n = experiments) significantly increases early vacuole formation as compared to control (n = 19), whereas Cdc42-N17 (n = 25) decreases it. (B) Representative images of ECFCs transfected with Cdc42-L61 and Cdc42-N17. White arrowheads indicate vacuoles. *P < 0.05, Scale bar = 50 μm	33
Figure 4.1	
Schematic diagram illustrating the effect on collagen stiffness on Cdc42 activation and vacuole formation.....	35

ABSTRACT

Kim, Seung Joon. M.S.B.M.E., Purdue University, August 2012. Effects of Collagen Gel Stiffness on Cdc42 Activities of Endothelial Colony Forming Cells during Early Vacuole Formation. Major Professor: Dr. Sungsoo Na.

Recent preclinical reports have provided evidence that endothelial colony forming cells (ECFCs), a subset of endothelial progenitor cells, significantly improve vessel formation, largely due to their robust vasculogenic potential. While it has been known that the Rho family GTPase Cdc42 is involved in this ECFC-driven vessel formation process, the effect of extracellular matrix (ECM) stiffness on its activity during vessel formation is largely unknown. Using a fluorescence resonance energy transfer (FRET)-based Cdc42 biosensor, we examined the spatio-temporal activity of Cdc42 of ECFCs in three-dimensional (3D) collagen matrices with varying stiffness. The result revealed that ECFCs exhibited an increase in Cdc42 activity in a soft (150 Pa) matrix, while they were much less responsive in a rigid (1 kPa) matrix. In both soft and rigid matrices, Cdc42 was highly activated near vacuoles. However, its activity is higher in a soft matrix than that in a rigid matrix. The observed Cdc42 activity was closely associated with vacuole formation. Soft matrices induced higher Cdc42 activity and faster vacuole formation than rigid matrices. However, vacuole area is not dependent on the stiffness of matrices. Time courses of Cdc42 activity and vacuole formation data revealed that Cdc42 activity proceeds vacuole formation. Collectively, these results suggest that matrix stiffness is critical in regulating Cdc42 activity in ECFCs and its activation is an important step in early vacuole formation.

1. INTRODUCTION

The vascular system provides nutrients and hormones and exchanges gases and the waste of cells to maintain homeostasis and respond in pathological conditions [1, 2]. Two essential mechanisms are involved in the formation of blood vessels: angiogenesis and vasculogenesis. Angiogenesis is the sprouting and growth of new capillaries from pre-existing vessels, whereas vasculogenesis is de novo formation of primitive vascular networks by the differentiation of endothelial precursor cells into endothelial cells (ECs) [2, 3]. Two processes allow the development of tissues over the diffusion limit of 100-200 μm [4, 5]. New capillaries, lined by endothelium, start to form where vascularization is needed to regenerate tissue and maintain homeostasis [6]. The remodeling of blood vessels continues when quiescent ECs are stimulated by cytokines so that the cells start to migrate, proliferate, differentiate, form lumens and lead to blood vessel stabilization in a sequence. During the remodeling process, vacuoles are formed inside the cytoplasm of the individual cells and then coalesce to form lumens (Fig. 1.1) [7, 8]. Vascularization is especially critical in both the progress of cancer and tissue engineering. Dr. Folkman has demonstrated that metastasis is dependent upon angiogenesis [9]. In addition, tissue engineering has still shown only limited success due to avascular structures which limit the diffusion of oxygen and nutrients to develop functional tissues [5]. Hence, understanding the molecular mechanisms that govern vascularization will provide the insight for therapeutic potentials for cancer, vascular diseases and the development of vascular tissue grafts.

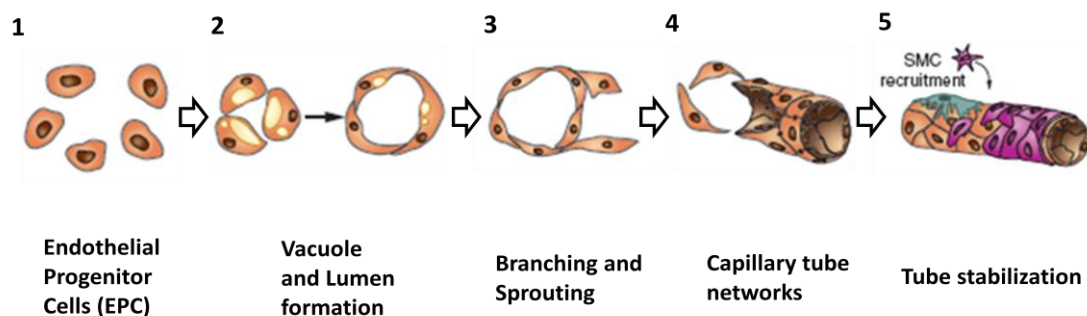


Figure 1.1 Morphogenetic steps of the remodeling blood vessels [8]

1.1 Endothelial Progenitor Cells in Vasculogenesis

To form a vascular network within scaffolds for therapeutic applications, implanted cells have to show both high proliferative ability and blood vessel forming ability. Various types of cells have been utilized to investigate in vitro capillary morphogenesis. Although human umbilical vein endothelial cells (HUVECs) have been shown to promote vasculogenesis and angiogenesis, they have showed limited capacity for proliferation [10-12].

Recently, endothelial progenitor cells (EPCs) have been identified as being released from bone marrow, circulate in the blood vessels and home to sites where vessel formation is needed [13]. The therapeutic potential of EPCs has already been shown to be quite promising for treatments. Therapeutic improvement has been shown as a cell therapy, as bioengineered grafts, a gene delivery and a clinical application [14]. Unlike mature ECs, EPCs have shown to improve neovascularization (Fig. 1.2) [15]. Although EPCs showed positive results in some clinical trials, their results were inconsistent. This is due to lack of specific markers to identify the EPCs, various isolation methods and the rarity of the cells [16-18].

Identification of putative EPCs has been based on surface markers of hematopoietic stem cells (HSCs) and ECs, such as CD34, CD133 and VEGFR2, von Willebrand factor (vWF), CD31, CD144 and C-X-C chemokine receptor type 4 (CXCR4).

While both hematopoietic and endothelial markers have been utilized to identify putative EPCs, the ambiguity of specific EPC markers has led to a difficulty in identification of putative EPC. There are two problems in isolation methods regarding the ambiguity of the EPC markers. EPCs may differentiate into mature ECs. Additionally, other cell populations such as hematopoietic stem cells, mature monocytes, dendritic cells and B lymphoid cells make it hard to discriminate putative EPC [19, 20]. Thus, developing specific markers for defining putative EPC is crucial to distinguish them from other subsets.

Regarding isolation methods, Asahara et al. first described the existence of EPCs [21]. Their report showed that peripheral blood mononuclear cells (MNCs) can be differentiated into mature ECs as well as putative EPCs, named as circulating angiogenic cells (CACs). These cells can incorporate into sites of neovascularization in animal models [22]. The isolated cells indicated as CACs showed the ability to uptake acetylated low-density lipoprotein (Ac-LDL) and bind ulex europaeus agglutinin 1 (UEA-1) [21, 22]. Additionally, CACs express cell surface markers such as CD31, CD144, vWF and kinase insert domain receptor (KDR) [22, 23]. However, this method has a critical defect because platelets putative EPCs. Thus, method is considered as an unreliable method to

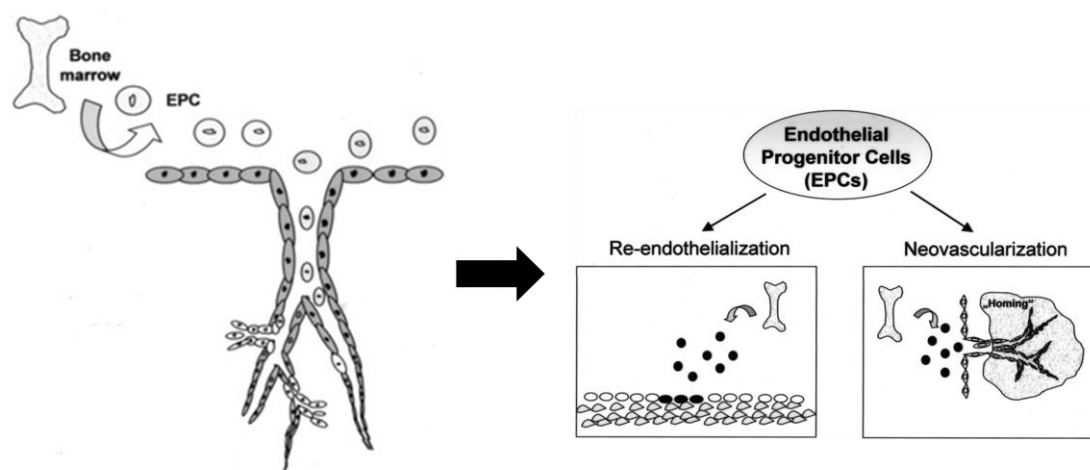


Figure 1.2 Schematic diagram of EPC homing and incorporation into tissue

contaminate MNCs so that platelet membrane proteins transfer to adherent this isolate putative EPCs [24].

The CACs isolating method has been modified by Hill et al. and referred to as colony-forming unit-Hill (CFU-Hill) [16]. CFU-Hill cells express same cell surface markers of CACs and show the ability to uptake Ac-LDL. CFU-Hill cells also express monocyte/macrophage cell surface markers such as CD14, CD45, and CD115. Furthermore, the cells ingested bacteria and displayed nonspecific esterase activity [23]. Although CFU-Hill cells contribute to neoangiogenesis, they are regarded as colonies of hematopoietic cells due to the lack of endothelial specificity [25].

The last isolating method is endothelial colony-forming cells (ECFCs) [18], which are also referred to as blood outgrowth endothelial cells (BOECs) [26]. ECFCs express CD31, CD105, CD144, CD146, vWF, and KDR as well as uptake Ac-LDL. Unlike CFU-Hill cells, ECFCs did not express hematopoietic/macrophage cell surface markers [25]. In addition, they demonstrated high telomerase activity and proliferative potential [18]. No other types of EPC have spontaneously formed the vasculature in vivo. Only ECFCs have a capacity to form a de novo vasculature in vivo and they have been speculated as an EPC [27]. Further analysis of specific markers and the functional vessel forming ability of EPC is needed to utilize the cell as a source of angiogenesis in a clinical application.

1.2 Matrices for in vitro Vasculogenesis

To build a bioengineered graft, a scaffold is necessary to provide suitable microenvironments for vascularization. A scaffold supports cell survival as well as cellular functions such as migration, differentiation and morphogenesis [28]. There are two types of polymers applied to a vasculature by ECs: synthetic- and nature-derived polymer. Synthetic matrices such as polyethylene glycol (PEG) [29] and poly (lactide-co-glycolide) (PLGA) [30] have been used to study endothelial capillary network formation.

Synthetic polymer matrices are appealing because they are controllable and reproducible. Most of synthetic polymers, however, can elicit the immune response [31] and degraded polymers can acidify the microenvironments which inhibit angiogenesis [32].

Natural-derived biopolymer matrices such as collagen, fibrin, matrigel, elastin, hyaluronic acid, dextran, fibronectin and alginite also have been studied in angiogenesis and vasculogenesis [13, 33-35]. The advantages of natural-derived biopolymer matrices are that they are bio-compatible, enzymatically degradable and their interaction with cells promotes vascularization [36]. The drawbacks of using natural-derived biopolymers are infection by pathogens, source and batch variation, and complicated systematic investigations of the matrix stiffness and biochemical signals which cannot be independently examined [37].

Specifically, collagen type I has been known to provoke vascular network formation of ECs. A substantial body of evidence has been provided that the interaction between collagens and ECs is relevant in capillary morphogenesis [28]. Also, collagen is highly occupied in tissues and showed the greatest mechanical integrity and broad range of mechanical properties [38, 39]. EC tubular morphogenesis is divided into cord formation and vascular lumen formation which depend on the culture types of a collagen gel. ECs form capillary-like cords in a 2-dimensional (2D) and 3-dimensional (3D) interstitial collagen gel, whereas cells form intracellular vacuoles and lumens in a suspension of a 3D collagen gel (Fig. 1.3) [40].

1.2.1 2D Scaffolds

A confluent monolayer of ECs with collagen [28], fibronectin [41] and fibrin [42] has been shown to form an interconnecting network of vascular cords. Collagen type I especially promotes vascular cord formation in a 2D and 3D interstitial gel. The mechanisms of how collagen type I supports cord-like structures have been identified. Collagen type I binds to $\alpha 1\beta 1$ and $\alpha 2\beta 1$ integrins and suppresses promotes cord

formation. On the other hand, the elevation of cAMP inhibits cord formation by ECs. In addition, Src kinase and Rho GTPase are involved in capillary cord formation via $\beta 1$ integrin. While activation of Src inhibits VE-cadherin to form actin stress fibers, inhibitors of Src and Rho suppress actin stress fiber induction so that capillary cord formation is disturbed [28]. These results suggest that actin stress fibers and contractility are critical in angiogenesis.

1.2.2 3D Scaffolds

EC tube morphogenesis has been investigated by a 3D gel which induces vacuoles and lumens. In a suspension of a 3D gel, including collagen, hyaluronic acid and fibrin, ECs tend to form intracellular vacuoles and lumens [28]. In a collagen gel, lumen formation is dependent on pinocytic intracellular vacuoles. These vacuoles coalesce with each other and form lumens [43]. Membrane type-matrix metalloproteinase (MT-MMP), Cdc42 and Rac1 are known to be required for vacuole and lumen formation. However, RhoA is not involved in the lumen formation in a 3D collagen model [44]. These results indicate cord formation and lumen formation by ECs depend on the distinctive matrix-integrin-cytoskeleton signaling pathway [28, 40].

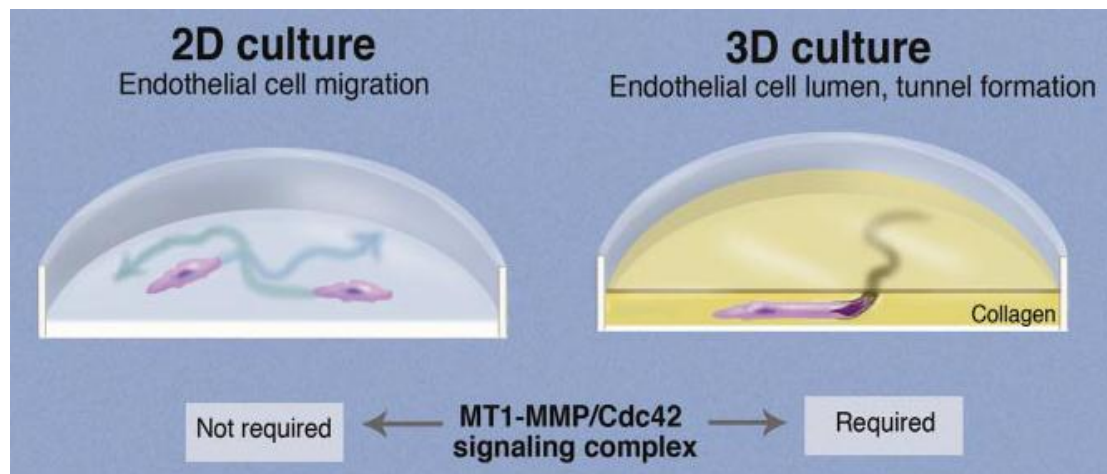


Figure 1.3 ECs in 2D culture form cord-like structure whereas ECs in 3D culture generate lumens [40]

1.3 Matrix Stiffness and in vitro Vasculogenesis

It has been well established that cells interact with microenvironments via focal adhesions. Focal adhesions are large molecular complexes that are composed of integrin receptors and multiple proteins including talin, vinculin and paxillin [45]. Mechanical cues from ECM are transmitted through focal adhesions to regulate cellular behaviors such as shape, migration, proliferation and differentiation [46]. The critical role of mechanical cues in cellular behaviors has been well revealed by stem cell studies. Ruiz et al. and Engler et al. have demonstrated that mechanical cues can control mesenchymal stem cell (MSC) lineage commitment [47, 48]. MSCs under high force differentiate into osteogenic lineage while the cells under low force differentiate into adipogenic lineage [47]. In addition, MSCs in a soft matrix differentiate into neuronal lineage, whereas matrices with intermediate and rigid stiffness induce muscular and osteogenic lineage, respectively [48]. Similarly, neural stem cells (NSCs) differentiate into neuronal lineage in a soft gel, but differentiate into glial lineage in a rigid gel [49]. Although the importance of mechanical cues from ECM and cellular behaviors has been verified with various types of evidence, capillary morphogenesis of ECs under mechanical properties of scaffolds has not been well understood.

1.3.1 Mechanical Properties of a 2D Gel in Vasculogenesis

The effect of ECM stiffness on vascular cord formation has been extensively studied [42, 50-52]. Califano et al. have provided the evidence that vascular cord formation is dependent on substrate mechanics [50]. Bovine aortic endothelial cells (BAECs) were cultured on various mechanical properties of substrates with type I collagen. Cord formation preferred a compliant substrate rather than a stiffer substrate. Despite of a stiffer substrate, the reduced density of collagen enabled the cells to form vascular cord. In addition, fibronectin was necessary to stabilize cell and cell contact and induce cord formation regardless of substrate stiffness [50]. Stéphanou et al. have demonstrated HUVECs on different concentrations of fibrin gels [42]. The results on the kinetics of vascular cord formation revealed that intermediate stiffness facilitated rapid

vascular cord formation. Flexible and rigid gels showed a limited and unstable vascular cord network [42].

Capillary morphogenesis by ECM density has been investigated by Ghajar et al. and Kniazeva et al. [51, 52]. They conducted an experiment to examine how HUVECs coated on micro-beads behave in different densities of fibrin gels. Both studies have revealed that increasing the density reduced capillary network formation. Ghajar et al. have concluded that the restriction of diffusion results in a reduced capillary network [51], whereas Kniazeva et al. have suggested that actin-mediated tractional forces regulate network formation [52]. These studies indicate that the mechanical property of ECM regulates capillary morphogenesis [51, 52].

1.3.2 Mechanical Properties of a 3D Gel in Vasculogenesis

In addition to cord formation and capillary morphogenesis, vascular lumen formation in a 3D gel under mechanical strain has been examined [34, 53-56]. Sieminski et al. seeded HUVECs and human blood outgrowth endothelial cells (BOECs) in floating and constrained collagen gels [53]. In this study, the elongation of network formation, lumen area and actin stress formation were shown to depend on cell type, collagen concentration and contractility of the gel. BOECs showed less lumen size than HUVECs while exerting more traction than HUVECs. In addition, larger lumen area in a rigid gel and an elongated network in a soft gel were observed. Together, these results suggest that the stiffness of the matrix and cell generated tension may play an important role in capillary morphogenesis [53].

Moreover, Yamamura et al. have investigated that bovine pulmonary microvascular endothelial cells (BPMECs) are seeded at collagen gels with varying mechanical properties [54]. In the flexible gel, a dense and thin network of small vacuoles was formed. In the rigid gel, larger lumens produced by multiple cells were formed. Because the cells need more degrading activity to penetrate the rigid gel, this

degrading activity may contribute to decreased the migratory activity and the formation of cell aggregates. In the flexible gel, on the other hand, the cell shifts to migratory activity rather than vascular morphogenesis so that small vacuoles are formed [54].

Hanjaya-Putra et al. have further demonstrated that in vitro tubulogenesis of EPC is regulated by both soluble cues and mechanical cues [34]. EPCs were cultured at three different Young's moduli, rigid, firm and yielding, of hyaluronic acid hydrogels and induced capillary morphogenesis by vascular endothelial growth factor (VEGF). In the yielding substrate, mean tube length, tube area and tube thickness were increased and open lumens were formed. These vascularization results were not shown in the rigid substrate. The results of yielding substrate suggest reduced tension between cells and ECM is sufficient to activate signals of vascular development. EPCs cultured on the rigid substrate, on the other hand, have to shift to producing MMPs to overcome ECM mechanical barriers instead of migration and morphogenesis [34].

Table 1.1 Summary of mechanical properties and vasculogenesis

Cell type	Stiffness	Morphogenetic type	Features	Ref.
BAEC	Collagen gel Young's modulus (200 ~ 10,000 Pa)	Capillary cord structure	Compliant substrate promotes the cord structure	[50]
HUVEC	Fibrin gel concentration (1, 2, 3 mg/ml)	Capillary cord structure	Intermediate rigidity promotes the cord structure	[42]
HUVEC	Fibronogen concentration (2.5, 5, 10 mg/ml)	Capillary network	Increasing density reduces the capillary network	[51]
HUVEC, HBOEC	Floating and constrained collagen gel (1.5, 3 mg/ml)	Lumen formation	Shorter and wider lumens in a constrained gel than a floating gel.	[53]
BPMEC	Collagen gel relaxation modulus (5000 ~ 23,000 Pa)	Lumen formation	Larger lumen is shown in a rigid gel	[54]
EPC	Hyaluronic acid-gelatin Young's modulus (10, 75, 650 Pa)	Lumen formation	Decreased substrate stiffness extends intracellular vacuoles	[34]
ECFC	Collagen gel Shear storage modulus (24, 136, 300 Pa)	Lumen formation	Increased stiffness decreases vacuole area	[55]
ECFC	Collagen gel concentration (0.5, 1.5, 2.5, 3.5 mg/ml)	Lumen formation	Higher concentration shows decreased density and increased total vessel area	[56]

Recently, Bailey et al. and Crister et al. seeded ECFCs in a different concentration of type I collagen gels and investigated the capillary morphogenesis in vitro and in vivo, respectively [55, 56]. Bailey et al. cultured ECFCs in both monomer and oligomer collagen gels with different collagen concentrations. Oligomer collagen showed the greatest vacuole density, similar vacuole areas and the greatest total vacuole area as compared to monomer collagen. At both oligomers and monomers, increased collagen concentration which increased the stiffness of the gel has decreased vacuole area due to spatial constraints imposed by increasing fibril density [55]. Crister et al. conducted the experiment of different mechanical properties of cellularized collagen matrices by ECFCs implanted into the flank of immunodeficient mice and investigated the capillary network formation. The density of ECFC-derived vessels was decreased, but total vessel area was increased in matrices with higher collagen concentration [56]. Taken together, these results support the notion that the stiffness of the matrix is a critical parameter to regulate angiogenesis and vasculogenesis of ECFCs.

1.4 Molecular Mechanisms of in vitro Vasculogenesis

EC lumen formation is an important event that occurs during vascular

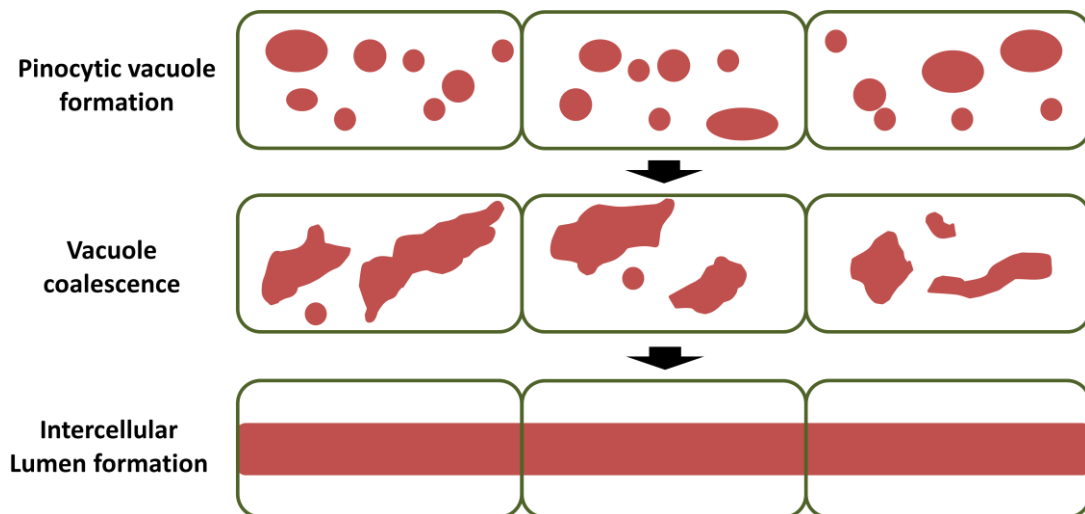


Figure.1.4 Model of vascular lumen formation and signal pathway [58]

morphogenesis. Many studies have attempted to define the pathway in vascular morphogenesis by ECs in 3D ECM environments, but it is still controversial. The first suggested model of vascular lumen formation is the pinocytic mechanism, which has been found to occur during intracellular vacuole formation in vitro models. Vacuoles arise from an invagination of the plasma membrane and subsequently coalesce to form a lumen (Fig. 1.4) [43, 57-58]. This process has been known to depend upon $\alpha 2\beta 1$ integrin, Cdc42, Rac1, and MT1-MMP that are needed for intracellular vacuoles formation by the pinocytic uptake of the plasma membrane mechanism [59].

1.4.1 Integrins in Vasculogenesis

Interaction between ECs and the ECM are required to form a vascular tube. Integrins are heterodimeric adhesion receptors and they have been recognized as a mediator of cell-matrix interactions [60, 61]. Nine integrins have been found to bind to collagen, laminins and fibronectins. Among these, $\alpha 1\beta 1$ and $\alpha 2\beta 1$ integrins are known as collagen-binding integrins that participate in vascular development [62]. Evidence for the participation of integrins in vascular lumen formation was proved by the inhibition of $\beta 1$ and $\alpha 2$, which results the interference in capillary formation. On top of that, the loss of the $\beta 1$ integrin has influenced the disruption of cell polarization and lumen formation as well as the decreased of Par3 protein levels [43, 60]. Also, treating cells with anti- $\alpha 2\beta 1$ antibody in order to activate the integrins has resulted in an increase of lumen formation [63].

1.4.2 Rho GTPases in Vasculogenesis

Rho GTPases, a member of the Ras superfamily of GTPases, include RhoA, Rac and Cdc42. These Rho GTPases regulate the cytoskeleton and connect the cytoskeleton and integrins [64]. Rho GTPases have prominent roles in various aspects of intracellular activities such as cell morphology, migration, contraction and secretory activity. Rho GTPases are bi-molecular switches by cycling between GDP and GTP states. Rho switch is regulated by activators which are named GEFs (Guanine nucleotide-exchange factors)

and suppressors which are GAPs (GTPase-activating proteins). GEFs exchange GDP to GTP and that leads to activation, whereas GAPs hydrolyse GTP to GDP and suppress activity [65].

Cdc42 is an important molecule of its function in actin polymerization and filopodia formation. Recently, Cdc42 has been known to regulate ECM remodeling in a 3D culture system. Depletion of Cdc42 in fibroblasts demonstrated reduced focal adhesions and a reduction in production of MMP that indicate Cdc42 is essential in ECM remodeling [66]. Rho and Cdc42 play an interacting role between cell-matrix by cellular morphology and matrix remodeling in a 3D culture [67].

Downstream proteins of the integrin signal pathway, Cdc42 and Rac1 are members of the Rho GTPase family that are also involved in vascular development [59]. Rho signaling pathways are also involved in various physiological functions in the maintenance of vascular homeostasis, such as vasoconstriction, hypertension, inflammation, and wound healing [68].

However, Cdc42 and Rac1 participated in vascular lumen formation. During the formation process, the activity of Cdc42 and Rac1 increases 2 to 2.5 folds [69] and Cdc42-specific guanine exchange factors, FGD4 and frabin, are also up-regulated two folds [59]. Additionally, it has been well demonstrated that inhibition of Rac1 and Cdc42 also inhibits the lumen formation [44]. Various downstream effectors of Rac1 and Cdc42 are activated as well. Pak2, Pak4, cell polarity proteins, which are Par3 and Par6, as well as PKC have been required for lumen and tube formation [69]. Later, PKC ϵ , Src, Yes, B-Raf, C-Raf and ERK1/2 also have been reported to be involved into EC lumen formation in 3D collagen gel [70]. Moreover, junction adhesion molecules Jam-B and Jam-C have been shown to be involved in lumen formation as proved by experiments utilizing siRNA and dominant-negative mutants (Fig.1.5) [71].

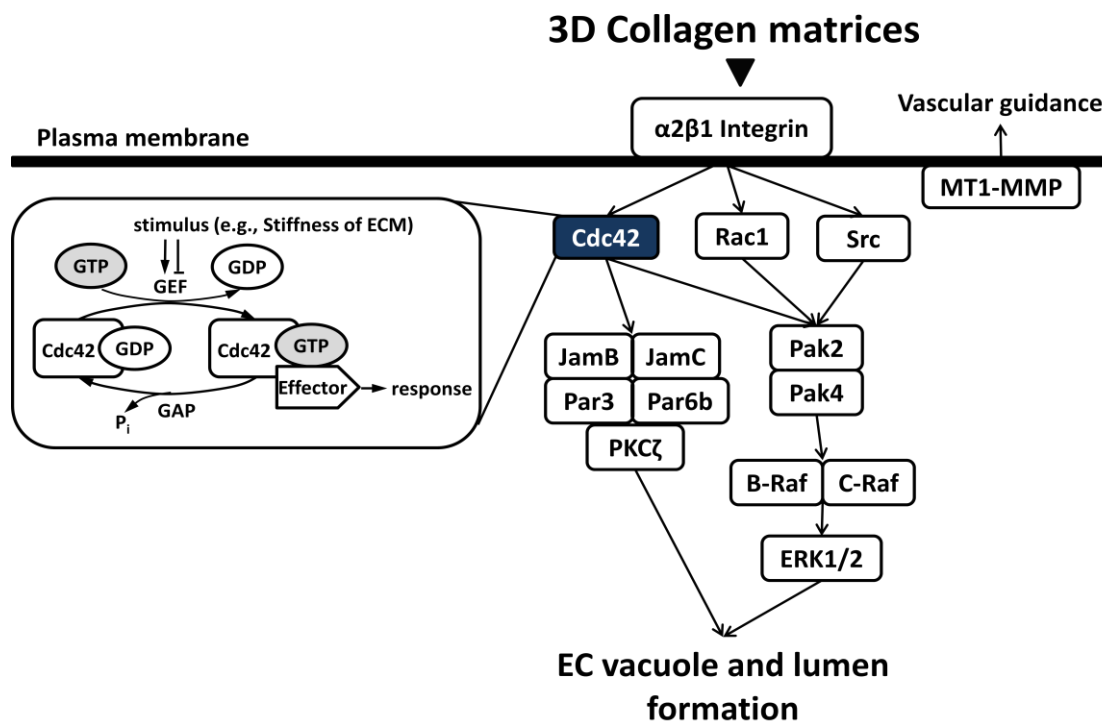


Figure 1.5 Signal pathway of vacuole and lumen formation [59, 69-71]

Many *in vitro* studies described the process of lumen formation. In 2006, the first *in vivo* research of vascular tube morphogenesis was conducted with zebrafish and showed how endothelial tubes assembled *in vivo*. The experiment was conducted by quantum dot injection and showed the transfer of quantum dots from the dorsal aorta to intersegmental ECs through vacuole uptake. The result indicates that intracellular and intercellular fusion of vacuoles drive the vascular lumen formation by exocytosis [58]. Later, the $\beta 1$ integrin and Par3 protein have been shown in the experiment conducted upon mice that they are required for endothelial polarity and lumen formation. Using gene knockout mice, ablation and blockade of $\beta 1$ integrin caused a loss of cell polarity and the inhibition of lumen formation. The report has suggested that $\beta 1$ integrin activation leads the activation and localization of Claudin-5, PECAM-1, VE-cdherin, and CD99 which are needed for lumen formation [60].

Although involvement of Cdc42 and Rac1 in vascular lumen formation has been proved by evidence, the role of RhoA is still controversial. Another possible mechanism

for vascular lumen formation has suggested that RhoA and Rho-associated protein kinase (ROCK) under VEGF signaling are involved with the evidence from the studies of intercellular junctions of blood vessels in the mice aorta [72]. Briefly, ECs adhere to each other and then separate by CD34-sialomucins which is localized by VE-cadherin. After that, Moesin localizes F-actin at the apical surface of the ECs. In a sequence, VEGF-A activates ROCK and makes non-muscle Myosin II. This enables ECs to separate apical EC surfaces and lead to EC shape change which causes vascular lumen formation. This report has suggested that lumen formation occurs via intercellularly [72]. However, the involvement of RhoA has been contradicted by other findings. Bayless et al., have provided the evidence that EC vacuole and lumen formation by pinocytosis is regulated by Rac1 and Cdc42, but RhoA has a minimal role. This has been proved by inhibitors; Toxin B, which blocked all of Rho GTPases, inhibited lumen formation but C3 transferase, which blocked only RhoA, did not interfere with lumen formation [44].

Recent studies have shown that cerebral cavernous malformation 2 (CCM2) affects Rho and Rap GTPases. CCM2 is not required in vasculogenesis but is needed in angiogenesis for the endothelium during mouse embryogenesis. CCM2 regulates lumen formation via the actin cytoskeleton, and the loss of functional CCM2 has been shown to lead to impaired lumen formation, increased actin stress fibers, and decreased barrier function, which is an indication of RhoA activation [73]. Moreover, Ras-interaction protein (RASIP 1) has been known to bind to the RhoA GTPase-activating protein (Arhgap29) and suppress RhoA activity. Loss of RASIP 1 or Arhgap29 results in an increase of RhoA activation, stress fiber and actomyosin so that the lumen formation is blocked. In addition, defects of RASIP1 increase RhoA/ROCK/myosin II activity by the blockade of Cdc42 and Rac1 signaling [74].

1.4.3 The Role of MT1-MMP in Vasculogenesis

The role of MT1-MMP has been investigated in vascular morphogenesis. It creates vascular guidance tunnels in the 3D collagen matrix. The modification of ECM

environments by ECs to support cellular functions is important in vascular morphogenesis. MMP is critical in all processes of angiogenesis: initiation, invasion and lumen formation of ECs. It is necessary to control vascular morphogenesis for re-growing and remodeling, for pericyte recruitment from the surrounding ECM, for basement membrane rearrangement and for vascular maturation and stabilization [28].

Also, tissue inhibitor of metalloproteinases (TIMPs) such as TIMP-2, TIMP-3 and TIMP-4 inhibit EC vacuole and lumen formation. In addition to the result, RNA knockdown of MT1-MMP markedly inhibits vacuole and lumen formation. However, soluble MMPs are not involved in vacuole and lumen formation. Only MMP-1 and MMP-10 appear in the regression of tube network [28].

1.4.4 Recent Findings of Molecular Pathways in Vasculogenesis

Recent *in vivo* experiments by zebrafish embryos have suggested that three distinct mechanisms of tube morphogenesis such as budding, cord hollowing, and cell hollowing coexist [75]. Moreover, a function of VEGF-driven angiogenesis is seen in the mice model. The co-activation of VEGF and Cdc42 improves capillary morphogenesis and lumen formation both *in vivo* and *in vitro* [76]. These reports have suggested that there are various pathways which depend upon various parameters, such as cell or matrix type. Another recent proposed mechanism of vasculogenesis formulated through the study of zebrafish has claimed selective sprouting and ECs migration toward erythrocytes is the pathway for angiogenesis. This model was supported by selective sprouting during the lumen formation. Ventral ECs migrated toward erythrocytes by VEGF-C via phosphoinositide 3-kinase and ephrin-B4 to surround the cell. Then, cells which formed lumens were retained by VEGF-A, which induced phospholipase- γ and ephrin-B2 [77]. These multiple possible mechanisms suggest that we only know the small portion of lumen formation signal pathway and that further analysis is required.

1.5 FRET Microscopy

For the detailed explanation of a protein function in living cells using fluorescent proteins, three methods have been developed to identify the dynamics of protein interaction: fluorescence resonance energy transfer (FRET), fluorescence correlation spectroscopy and complementation of split fluorescent proteins [78]. Among these techniques, FRET has been the most commonly used to investigate the function of protein in living cells. The principle of FRET is two fluorophores are fused as a donor and acceptor. When activation of a probe allows two fluorophores close to shorter than 10 nm in proximity by the conformational changes, a donor fluorophore can transmit energy into an acceptor fluorophore. This causes the acceptor fluorophore to fluoresce its emission spectrum [78].

1.5.1 Rho GTPases Biosensors based on FRET

To understand spatiotemporal activity of Rho GTPases, Dr. Matsuda's group has developed the FRET probes of Rho GTPases (Fig. 1.6) [79-81]. The probe consists of four domains: a donor (CFP), an acceptor (YFP), the GTPases and the GTP binding domains and are sequentially connected. Between domains, spacer is needed. Spacer consists of repeated sequences glycine (Gly) and serine (Ser). Gly is for flexible folding whereas Ser is for preventing aggregation. In the inactive state, GDP binds to GTPases so that CFP and YFP probes are placed remotely and fluorescent emission is exclusively from CFP. In the active state, GDP is changed to GTP, causing conformational changes in the probe that bring CFP and YFP to sufficient proximity of energy transfer. The measurement of YFP/CFP ratio corresponds to GTP/GDP ratio so that we can track changes in protein activity [79].

The Matsuda's group has developed Rac1, Cdc42 [80] and RhoA [81] FRET-based probes. Although GFP-based FRET probes are classified into intermolecular and intramolecular probes, Raichu-GTPases are intramolecular probes. By using Raichu-Rac1 and Raichu-Cdc42 probes, spatiotemporal activity was investigated during cell migration.

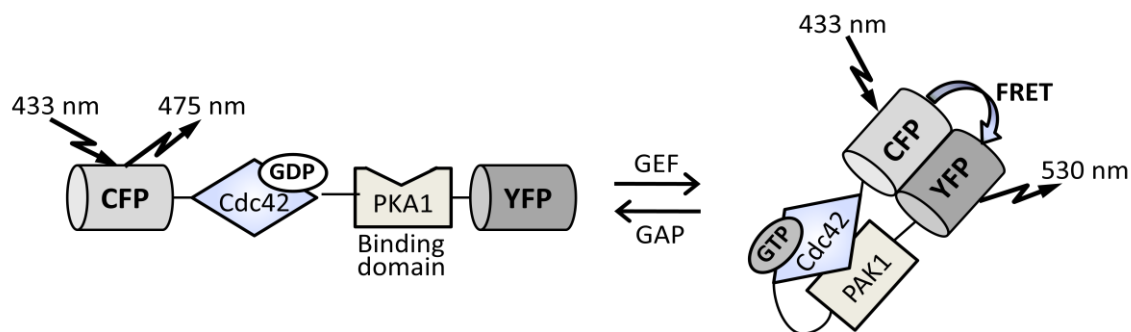


Figure 1.6 Structure of FRET-based Cdc42 biosensor [79]

The results showed that Rac1 was highly activated at the rear edge whereas Cdc42 was highly activated at the leading edge [80]. By including a RhoA probe, they also monitored spatiotemporal activity during cell division. Temporally, GTPases were highly activated in interphase but decreased during the mitotic phase. Spatially, RhoA activity was highly detected at cleavage furrow. Also, Rac1 was highly activated at the polar sides after telophase and Cdc42 was high at the membrane in cytokinesis [81]. These reports showed FRET-based probes can be used to visualize GTPases regulation in diverse aspects of cellular behaviors.

1.5.2 Optical Setup of Microscopy

To measure spatiotemporal protein interactions of a living cell in 3D culture, widefield and confocal microscopes have been utilized. Thus, appropriate optical setup of the experiment is also required to visualize fluorescent proteins. The appropriate microscope and objective are needed. The light source is a halogen or xenon lamp used for fluorescent images. Firstly, neutral density (ND) filters are used to reduce the intensity of excitation light. Three filters are needed: a CFP (donor) excitation filter, a CFP (donor) emission filter and an YFP (acceptor) emission filter. These filters are located at two wheels which enable filters to rapidly switch. The emission filter wheel is located next to CCD camera. 3D stack images can be acquired by the motorized stage with a controller (Fig. 1.7) [82].

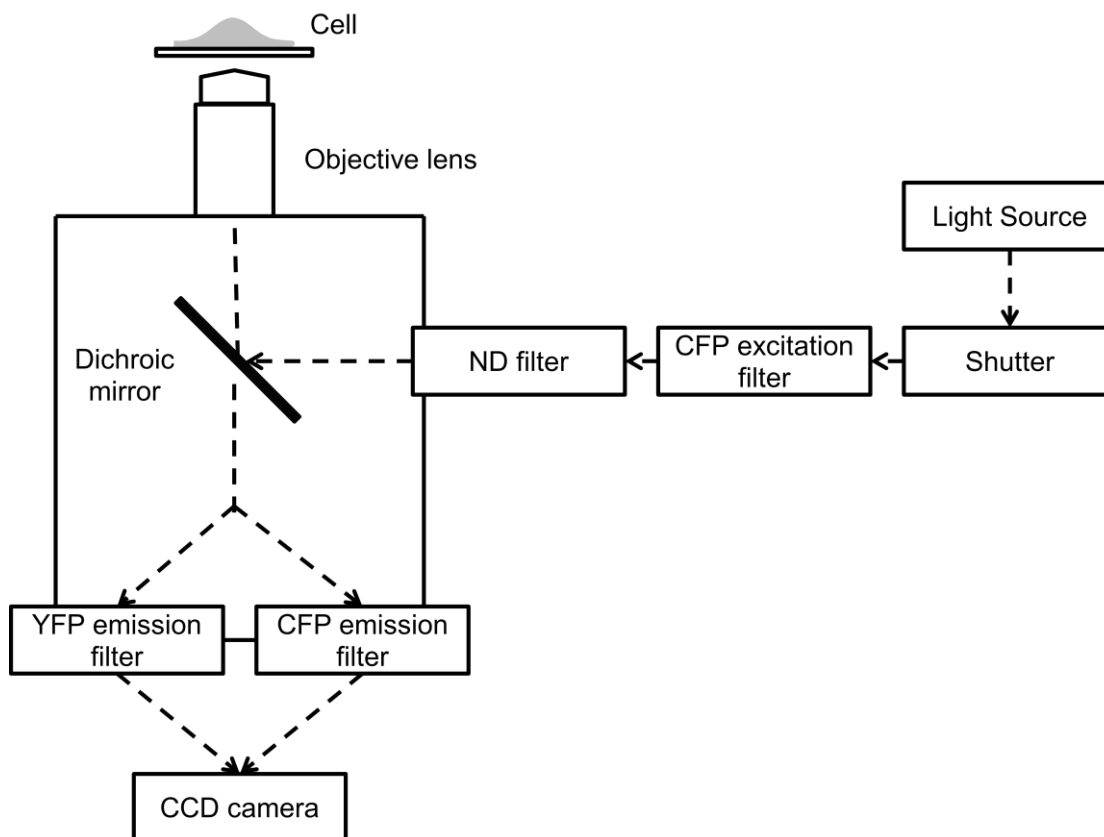


Figure 1.7 The outline of optical setup of the FRET microscope system [82]

1.6 Thesis Objectives

The objective of this dissertation is to elucidate the role of matrix stiffness in regulating the capillary morphogenesis. To be specific, the effect of altered matrix stiffness in Cdc42 activation and in vitro vacuole formation of ECFCs was examined. There are two specific goals in this dissertation.

The first goal is to uncover the spatiotemporal activity of Cdc42, linking to matrix stiffness during early vacuole formation. In this regard, vacuole formation and Cdc42 activity of ECFCs was investigated under shear storage moduli of 150 Pa and 1 kPa. To measure spatiotemporal Cdc42 activity, we used Cdc42 FRET-based probe which enables us to observe protein functions in a living cell.

The second goal is to explore the contribution of the Cdc42 activation in the kinetics of vacuole formation and vacuole size. In order to assess the role of Cdc42 activation, Cdc42 mutants were used.

2. METHODS

2.1 Cell Maintenance

ECFCs, isolated from human umbilical cord blood, were obtained from Dr. Yoder (Indiana University School of Medicine, Indianapolis, IN) and cultured under previously described method [18]. Briefly, ECFCs were cultured in EGM-2 media (Lonza, Walkersville, MD) supplemented with 10% of defined FBS (Invitrogen, Carlsbad, CA) and 1.5% of antibiotic-antimycotic (Invitrogen, Carlsbad, CA), and maintained at 37 °C and 5% CO₂ in a humidified incubator. Prior to experiments, the cells were cultured in a T-75 tissue culture flask (Becton, Dickinson and Co., Franklin Lakes, NJ), coated with 50 µg/ml of rat-tail collagen type I (BD Biosciences, Franklin Lakes, NJ), and passages 4 to 9 were used for all experiments.

2.2 DNA Plasmids and Transfection

We used a FRET-based, cyan fluorescent protein (CFP)-yellow fluorescent protein (YFP) Cdc42 biosensor, a generous gift from Dr. Matsuda (Kyoto University, Japan). Its characteristics and specificity were well described [80]. As Cdc42 mutants, a constitutively-active Cdc42 (Cdc42-L61) and a dominant-negative Cdc42 (Cdc42-N17) were used. The DNA plasmids were transfected into the cells using a Neon transfection system (Invitrogen, Carlsbad, CA) following the manufacturer's protocol. A single, 1000 mV pulse with duration of 20 ms was found to be an optimal parameter for transfection.

Table 2.1 Summary of shear storage modulus of collagen matrices by the collagen polymerization composition.

Approx. Conc. (mg/ml)	Final Stiff. (Pa)	Final Vol.(ml)	HCl(ml)	Collagen(ml)	PBS(ml)	NaOH(ml)	CaCl ₂ (ml)
0.382551	10	0.5	0.357	0.03	0.05	0.05	0.013
1.313373	100	0.5	0.283	0.104	0.05	0.05	0.013
1.584185	150	0.5	0.262	0.126	0.05	0.05	0.013
1.810423	200	0.5	0.244	0.144	0.05	0.05	0.013
2.782277	500	0.5	0.167	0.221	0.05	0.05	0.013
3.478689	800	0.5	0.111	0.276	0.05	0.05	0.013
3.870521	1000	0.5	0.08	0.307	0.05	0.05	0.013

2.3 Fabrication of Collagen Gel

The collagen mixture was provided by Dr. Voytik-Harbin (Purdue University, West Lafayette, IN) and followed the preparation as previously described [39]. The mixture included porcine skin collagen (6.8 mg/ml), 0.01 N HCl, 10x PBS, 0.1 N NaOH and CaCl₂ to achieve neutral pH. The stiffness of collagen gel was measured using a stress-controlled AR2000 rheometer (TA Instruments, New Castle, DE) [39]. The shear storage modulus (G' , stiffness) of 150 Pa was 1.58 mg/ml and that of 1 kPa was 3.87 mg/ml (Fig 2.1, Table 2.1). To solidify the mixture, gel was incubated at 37 °C and 5% CO₂ for 30 min.

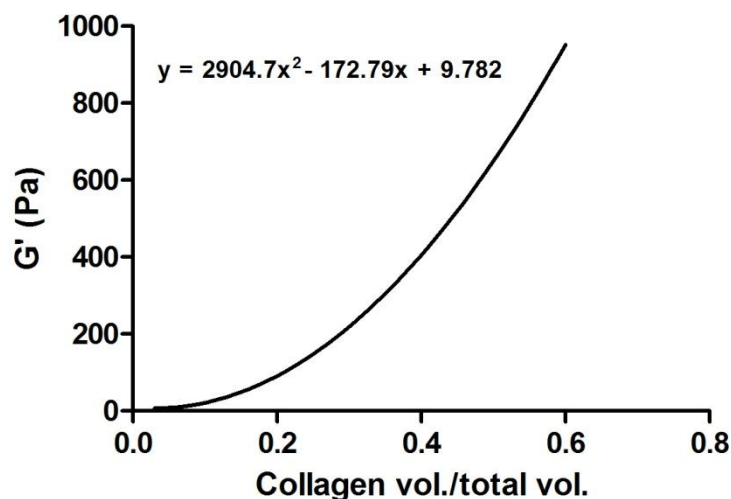


Figure 2.1 The relationship between shear storage modulus and collagen quantity [39]

2.4 In vitro Early Vacuole Formation Model

A small glass cylinder (Fisher Scientific, Pittsburgh, PA) was placed on top of 35 mm glass-bottom dish (MatTek Co, Ashland, MA). ECFCs transfected with Cdc42 biosensors were mixed with collagen solution in the cylinder and incubated at 37 °C and 5% CO₂ for 30 min. In order to induce vacuole formation, we followed the published method [83, 84]. First, ECFCs were incubated overnight in EBM-2 media (Lonza, Walkersville, MD) containing 40 ng/ml of fibroblast growth factor (FGF-2, R&D systems, Minneapolis, MN) and reduced-serum II supplement (RS II, 1:250) to maintain the cell viability and prime the vacuole formation. At the time of experiments, media was replaced with fresh EBM-2 media supplemented with 200 ng/ml of stem cell factor (SCF), stromal cell-derived factor-1 α (SDF-1 α), and interleukin-3 (IL-3) (R&D systems, Minneapolis, MN) to induce vacuole formation (Fig. 2.2) [83]. RS II was prepared by the published protocol (Fig. 2.3) [84].

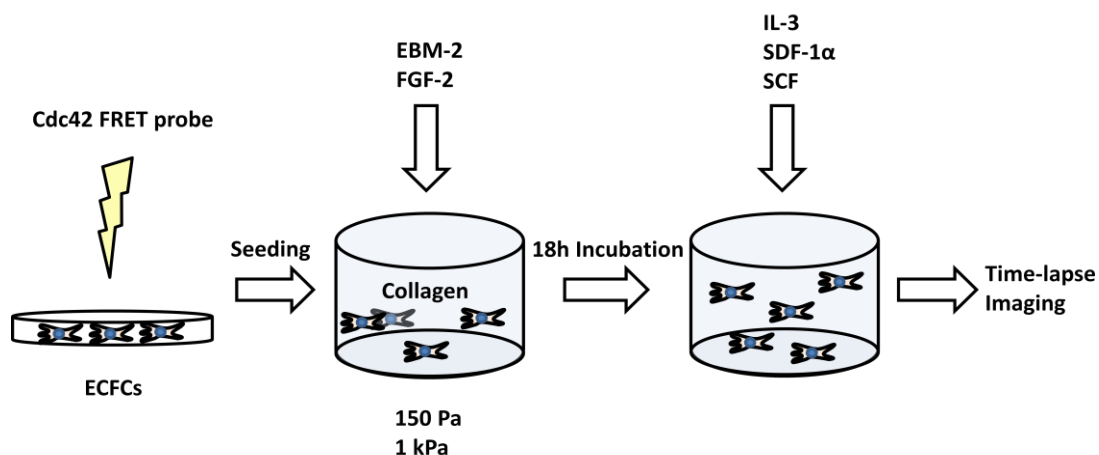


Figure 2.2 Schematic diagram of experimental procedure

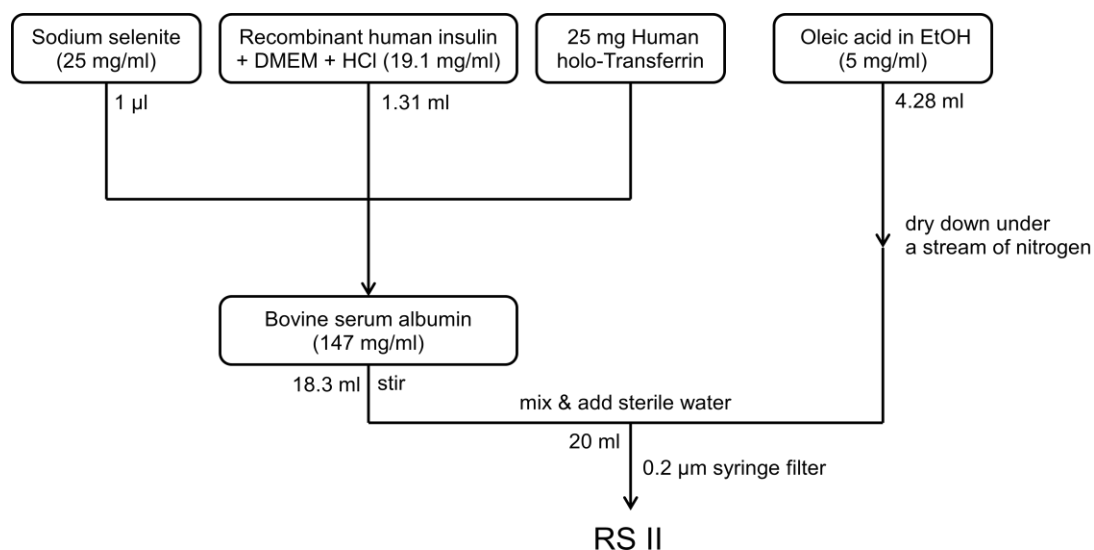


Figure 2.3 Flow chart of the preparation RS II [84]

2.5 FRET Microscopy

All images were obtained by using an automated fluorescence microscope (Nikon, Melville, NY) equipped with an electron-multiplying charge-coupled device (EMCCD) camera (Photometrix, Tucson, AZ), a filter wheel controller (Sutter, Novato, CA), and a perfect focus system (PFS; Nikon, Melville, NY). The following filter sets are used (Semrock, Rochester, NY): CFP excitation: 438 nm / 24nm (wavelength/bandwidth); CFP emission: 483 nm / 32 nm; YFP (FRET) emission: 542 nm / 27 nm. Cells were illuminated with a 100 W Hg lamp through an ND64 (~1.5% transmittance) neutral density filter to minimize photobleaching. Time-lapse images were acquired at an interval of 1 h with a 40X (0.75 numerical aperture) objective. Z-stack images were acquired at 0.6 µm intervals. FRET images for Cdc42 activity were generated with NIS-Elements software (Nikon, Melville, NY) by computing emission ratio of YFP/CFP for the individual cell. During imaging, the cells were maintained at 37 °C using an air stream incubator (Nevtek, Williamsville, VA).

2.6 Image Processing

Acquired images (512 x 512 pixels, 0.4 μ m/pixel) were analyzed by both NIS Elements software and ImageJ software (NIH, Bethesda, MD). In NIS Elements, selected images were background-subtracted. FRET images were displayed by the ratio of YFP/CFP with a pseudo-colored scale. Z-stack images were used to generate 3D-projection images. ImageJ software was used to display pseudo-colored FRET images [85]. First, both CFP and YFP images were background-subtracted by the rolling ball algorithm. Both images were aligned pixel to pixel and changed to 32 bit version. Smooth filter was applied to reduce the noise and threshold adjustment was carried out to eliminate artifacts by the noise. Corresponding pixels in the aligned CFP and YFP images were computed to generate YFP/CFP ratio images and a pseudo-colored scale was generated by Blue_Green_Red lookup table (Fig. 2.3) [85]. Hot color indicates higher activation of Cdc42 whereas cold color lower activation.



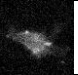
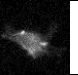
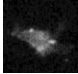
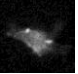
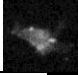
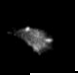

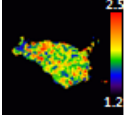
Processing Step	ImageJ Command	Outcome	
		CFP	YFP
Select ROI to be analyzed and crop the images	Edit>Selection>Specify images >Crop		
Background correction	Process>Subtract background (Rolling ball radius)		
Registration	Plugins>Registration> MultistackReg		
32-Bit conversion	Image>Type (32_bit)		
Smooth filter	Process>Smooth		
Threshold (only YFP)	Image>Adjust>Threshold (Default, B&W, Dark background)		
Ratio YFP/CFP	Plugins>Ratio plus		
LUT assignment	Plugins>NucMed>Lookup Tables (Blue_Green_Red)		
Range adjustment	Image>Adjust >Brightness/Contrast		
Preparation image for presentation	Image>Type (RGB color)		

Figure 2.4 The procedure of FRET ratio image generation by using the ImageJ software [85]

2.7 Data Analysis

Time courses of Cdc42 activity was quantified with the emission ratio of YFP/CFP. The emission ratios were averaged over the whole cell and were normalized to time point 0 h. The spatial analysis of Cdc42 activity was conducted by ImageJ software. A line was drawn on the body of cell including vacuoles. The plot profile represents the FRET intensity along the line [86]. The kinetics of vacuole formation was determined by the time point when vacuole was formed. DIC images were used to measure the vacuole area. For statistical analysis, outliers were deleted based on the Chauvenet's criterion using the MATLAB program (Mathworks, Natick, MA).

2.8 Statistical Analysis

Data were presented as the mean \pm standard error of the mean (SEM). In order to verify the statistical significance, one-way ANOVA was applied to the time course of Cdc42 activity and unpaired t-test was used for vacuole area analysis using Prism 5 software (Graphpad Software, La Jolla, CA). P-value less than 0.05 was considered as a significant difference.

3. RESULTS

3.1 Time-Lapse Imaging of ECFC Vacuole Formation in 3D Collagen Matrices

A significant body of evidence has provided the role of Cdc42 and collagen gel in vacuole formation, but little is known about the spatiotemporal activity of Cdc42 during vacuole formation at the subcellular resolution. To examine the activity of Cdc42 during early vacuole formation, ECFCs, transfected with Cdc42 FRET-based biosensor, were seeded at a density of 1×10^7 cells/ml in 3D collagen matrices with two different shear storage moduli. For this study we used two stiffness values, 150 Pa and 1 kPa.

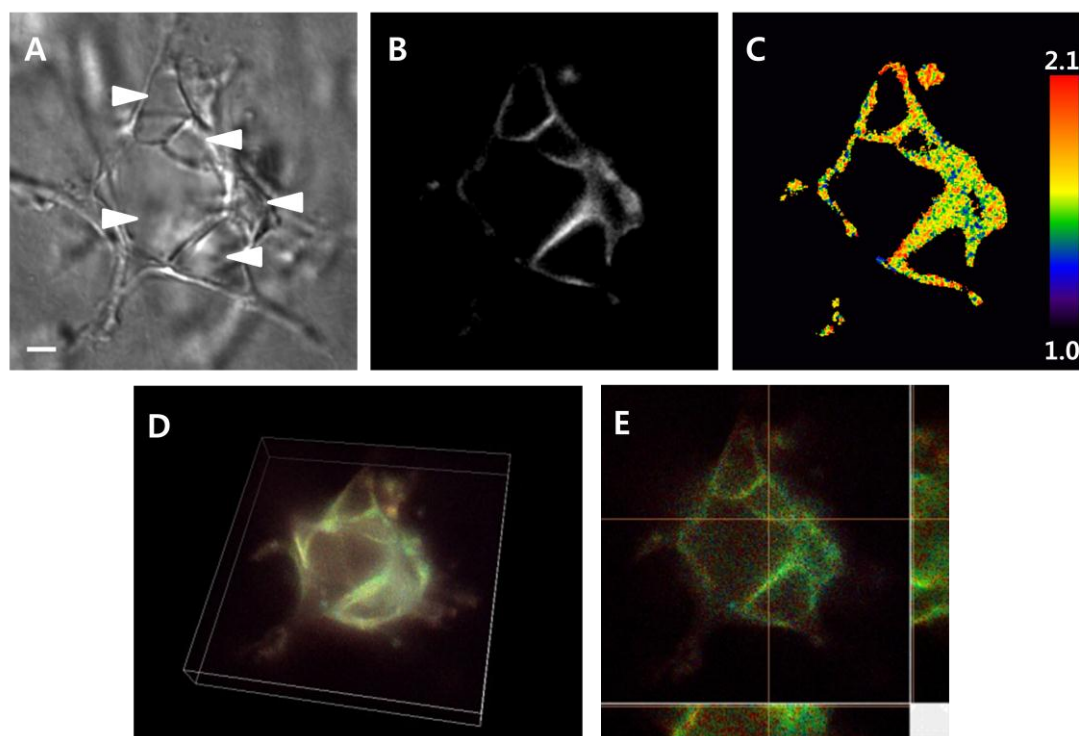


Figure 3.1 Representative images of vacuole forming cells. (A) DIC, (B) YFP, (C) YFP/CFP emission ratio image, (D) 3D-projection image (E) z-stack orthogonal images. White arrowheads indicate vacuoles. Scale bar = 10 μ m

To study Cdc42 activation during early vacuole formation, we modified previous method [83, 84]. Instead of adding FGF-2 into collagen matrices, we added 40 ng/ml of FGF-2 into EBM-2 media and incubated overnight with 40 ng/ml of FGF-2 to up-regulate hematopoietic cytokine receptors. In our vasculogenesis model, vacuoles were formed within 6 h and they were enlarged and coalesced (Fig. 3.1). The occurrence of vacuole indicates that our modified assay is suitable to study early vacuole formation. More importantly, we observed that high Cdc42 activation occurred at vacuole sites, suggesting the involvement of Cdc42 in early vacuole formation.

3.2 Cdc42 is Activated at Vacuole Sites

We examined the localization of Cdc42 during vacuole formation. Previous studies have provided the evidence of Rho GTPases localization during migration [86, 87] and neurite extension [88]. Here, we demonstrated that Cdc42 is localized at vacuole sites. The lateral view of Cdc42 localization showed that Cdc42 is consistently activated along the z-levels (Fig 3.1). In addition, FRET ratio profile along the line across the vacuole and cell body was analyzed. In both soft and rigid matrices, high activation of Cdc42 was observed adjacent to vacuole sites (Fig. 3.2). The localization of Cdc42 near vacuole sites provides the evidence of its importance in vacuole formation.

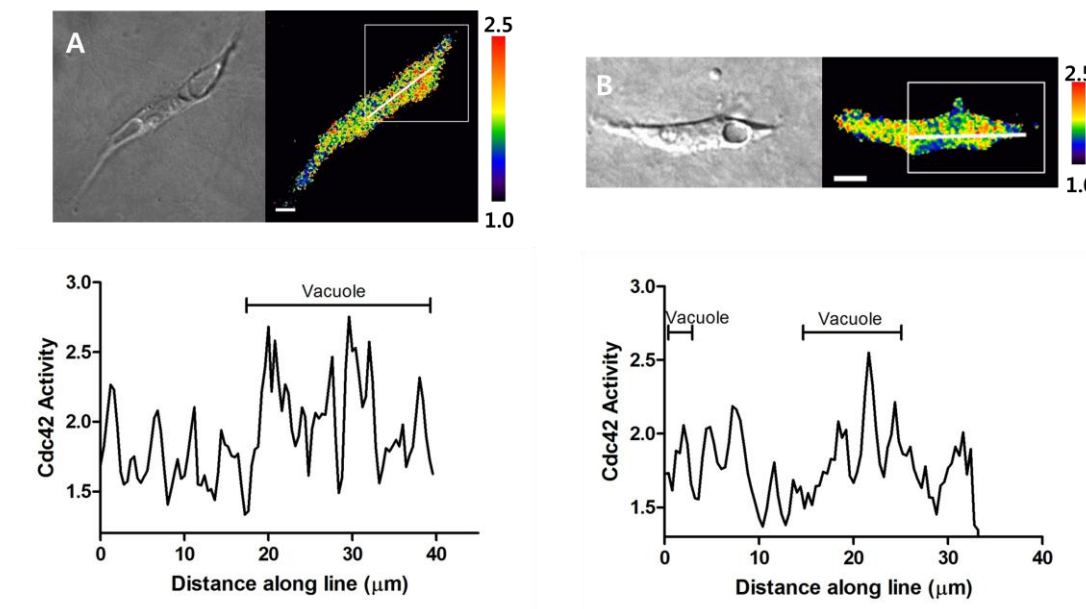


Figure 3.2 Plot profile of Cdc42 activity along the line on the cell body. The graph shows that Cdc42 activation is highly activated in both (A) soft (150 Pa) matrices and (B) rigid (1 kPa) matrices. Scale bar = 10 μm

3.3 Cdc42 Activity is Increased in Soft Matrices during Early Vacuole Formation

It has been well established that Cdc42 is associated with capillary morphogenesis in collagen gel matrix [44, 59], and plays an important role in mechanotransduction [67, 89]. To determine the role of the stiffness of matrix on Cdc42 activity during early vacuole formation, we transfected a Cdc42 biosensor into ECFCs and measured Cdc42 activity near vacuole sites for 9 h (Fig 3.3). In soft (150 Pa) matrices, Cdc42 activity was increased (12.37 %) rapidly until 3 h (Fig 3.4). However, in rigid (1 kPa) matrices, significant Cdc42 activity was not observed during vacuole formation (Fig. 3.4). This result suggests that stiffness of collagen matrices are involved in Cdc42 activation during early vacuole formation.

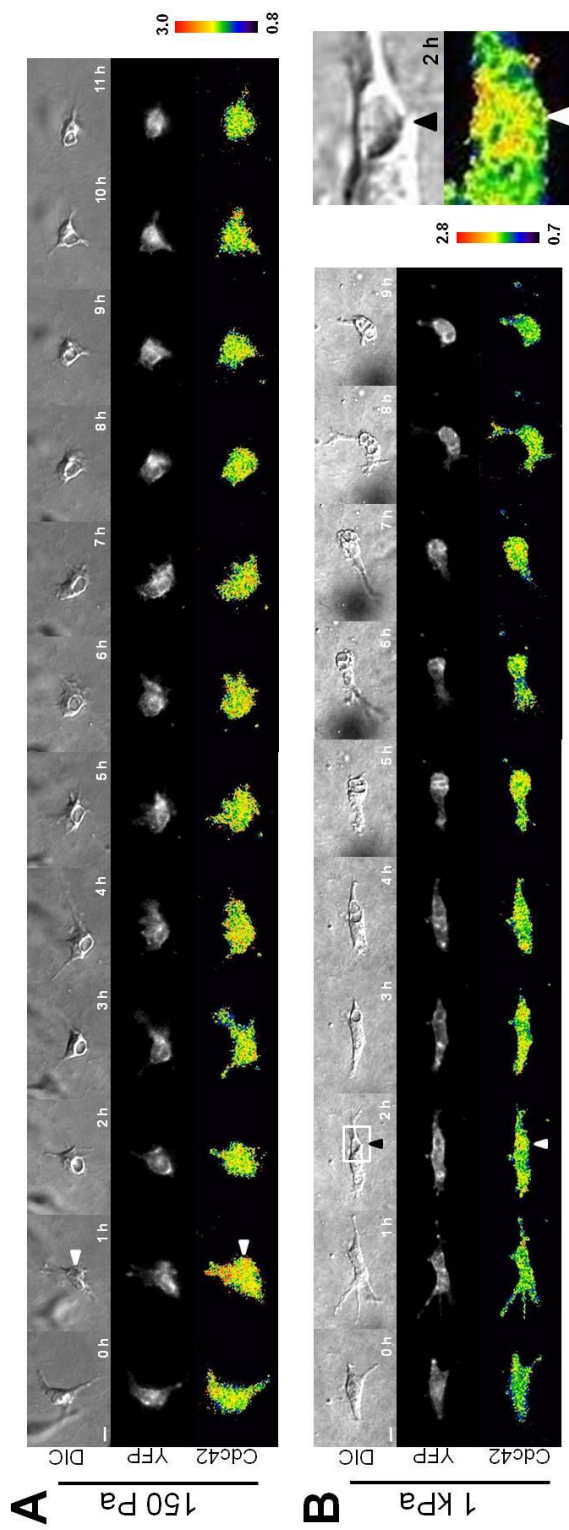


Figure 3.3 Time-lapse images of ECFCs during early vacuole formation. (A) Vacuole is formed at 1 h after cytokines treatment in soft (150 Pa) matrices and Cdc42 is highly activated near vacuole area. (B) Vacuole is formed at 2 h after cytokines treatment in rigid (1 kPa) matrices. Right-bottom enlarged image shows high Cdc42 activation near vacuole area. Color bars represent emission ratio of YFP/CFP of the biosensor, an index of Cdc42 activation. Images of YFP/CFP are scaled according to the corresponding color bars. The white boxes are cropped and enlarged for better visualization. White and black arrowheads indicate vacuoles in all figures. Scale bar = 10 μ m

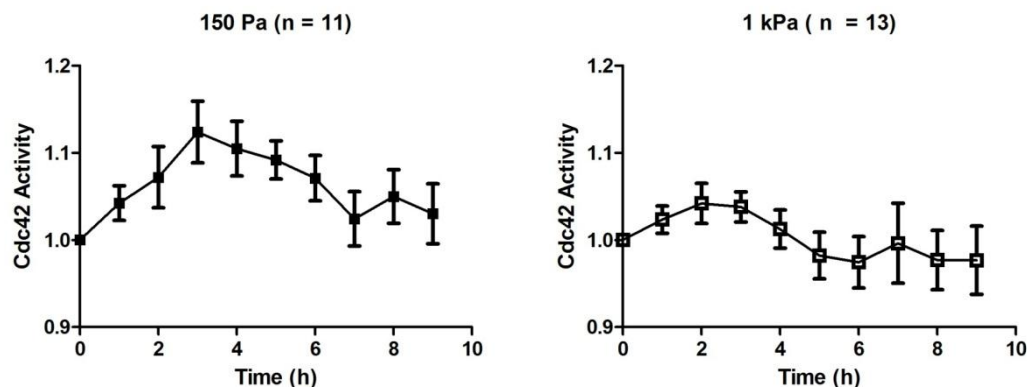


Figure 3.4 Time courses of Cdc42 activation during early vacuole formation. Cdc42 is highly activated at 3 h in soft (150 Pa) matrices during early vacuole formation. Time courses of YFP/CFP emission ratio are averaged over the whole cells and normalized to time point 0 h. Data represent mean \pm SEM.

3.4 Vacuoles were Formed Earlier in Soft Matrices than in Rigid Matrices

To determine the role of matrix stiffness on the kinetics of vacuole formation, we quantified the number of cells that made vacuoles for 6 h. This is the first detailed report of how matrix stiffness contributes to the kinetics of early vacuole formation. Soft matrices induced earlier vacuole formation (62.5 % within 3 h), while rigid matrices led

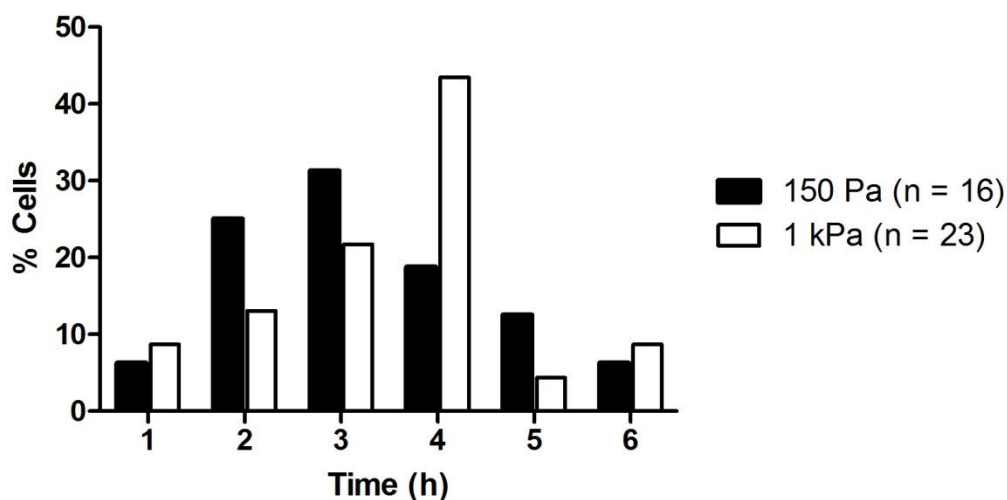


Figure 3.5 The kinetics of early vacuole formation. Vacuoles formed earlier in soft matrices than rigid matrices.

to slower vacuole formation (43.48 % at 4 h) (Fig. 3.5). These results suggest that the stiffness of matrix affects the kinetics of early vacuole formation.

3.5 Vacuole Area is not Dependent on Matrix Stiffness

Previous reports have demonstrated that increasing the stiffness of 3D collagen matrices decreases the vacuole area of ECs [34, 55]. The results revealed that average vacuole area in soft matrices is larger ($106.1 \pm 7.787 \mu\text{m}^2$) than that ($100.3 \pm 7.809 \mu\text{m}^2$) in rigid matrices (Fig. 3.6). These results are consistent with previous reports of Hanjaya-Putra et al. [34] and Bailey et al. [55] demonstrating that reduced stiffness increases vacuole area. However, our results in two different matrices did not show a significant difference.

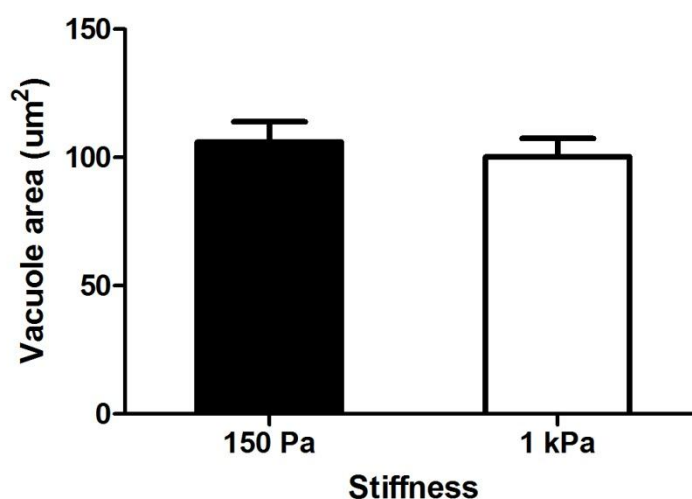


Figure 3.6 The effect of matrix stiffness on vacuole area. Vacuole area is not dependent on matrix stiffness. Soft matrices (n = 46, n = cells) and rigid matrices (n = 49) do not show a significant difference. Data represent mean \pm SEM.

3.6 Early Vacuole Formation is Mediated in Part by Cdc42

To further examine the role of Cdc42 activity in early vacuole formation, we co-transfected ECFCs with GFP-actin and one of Cdc42 mutants, a constitutively active Cdc42-L61 and a dominant negative Cdc42-N17. The control was only transfected with a GFP-actin. Only transfected cells (confirmed by GFP) were quantified after 4 h of hematopoietic cytokines treatment (Fig. 3.7). The results showed that 15 % of ECFCs formed vacuoles in control (14.77 ± 0.03 %, $n = 19$, $n =$ the number of experiments) and Cdc42-L61 significantly increased vacuole formation (24.28 ± 0.027 %, $n = 20$). Although less vacuoles (10.86 ± 0.027 %, $n = 25$) were formed in Cdc42-N17-transfected ECFCs, dominant negative Cdc42 failed to completely block the vacuole formation (Fig. 3.8). These results suggest that other factors, independent of Cdc42, may also participate in regulating ECFC vacuole formation.

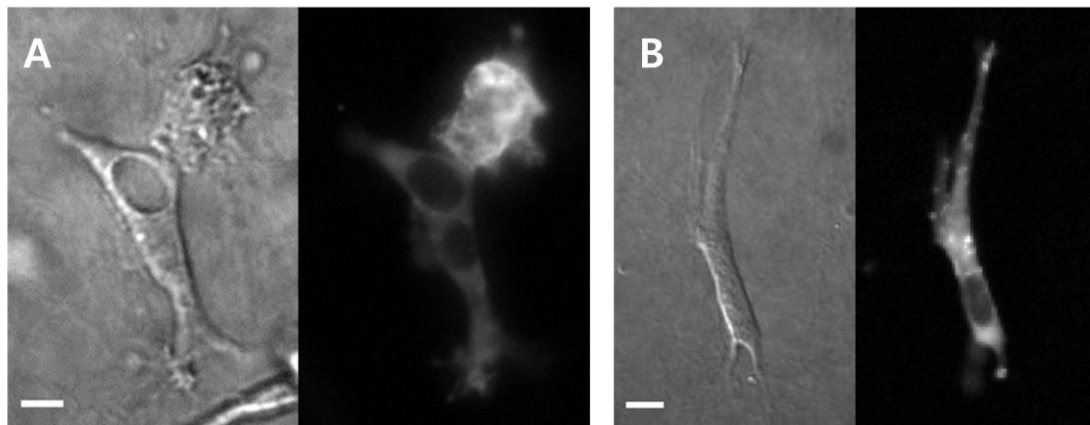


Figure 3.7 Expression of GFP-actin by mutants transfected ECFCs. (A) Cdc42-L61 promoted vacuole formation while transfection with (B) Cdc42-N17 inhibited vacuole formation. Scale bar = 10 μ m

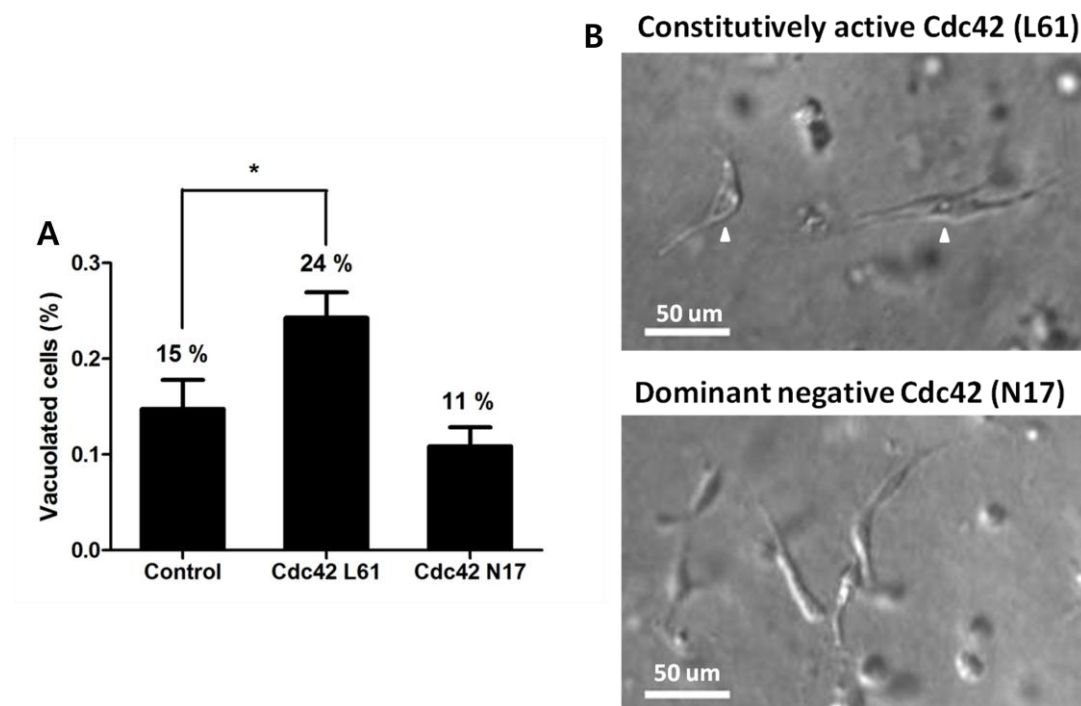


Figure 3.8 The effect of Cdc42 on vacuole formation. Early vacuole formation is mediated in part by Cdc42. (A) Treatment of Cdc42-L61 (n = 20, n = experiments) significantly increases early vacuole formation as compared to control (n = 19), whereas Cdc42-N17 (n = 25) decreases it. (B) Representative images of ECFCs transfected with Cdc42-L61 and Cdc42-N17. White arrowheads indicate vacuoles. *P < 0.05, Scale bar = 50 μ m

4. DISCUSSION

Vascularization, driven by EPCs, is essential for tissue survival and development of a functional bioengineering graft. It is known that ECFCs, a subset of EPCs, have a great therapeutic potential in repair of damaged tissues [15, 18, 56]. While substantial progress has been made to uncover the mechanism of vascularization using ECFCs, it remains elusive how individual ECFCs respond to the rigidity of the matrix spatially and temporally to regulate vacuole formation.

Previous works have demonstrated a role of cell-matrix interaction in capillary morphogenesis [34, 42, 50-56]. ECs form capillary cord sprouting in 2D and 3D interstitial gels, while hollowing of individual cells is shown in 3D gels [28, 40]. This hollowing is known to generate vacuoles in the cytoplasm through the pinocytic process. Vacuoles then coalesce and connect to form lumen with adjacent cells [57, 58]. It has been shown that the process of capillary morphogenesis in 3D model depends on the matrix-integrin-cytoskeleton signaling axis [28]. This axis has demonstrated the involvement of Rho family GTPases such as Rac1 and Cdc42, and MT1-MMP in lumen formation [59]. Inhibition of Cdc42 and Rac1 decreases lumen formation, suggesting a significant role of Rho family GTPases in capillary morphogenesis [44]. Thus, it is obvious that Cdc42 is involved in both mechanotransduction via ECM and the capillary morphogenesis pathway. Although Cdc42 is obviously involved in vacuole formation in 3D matrices, it is not known whether Cdc42 activity is altered by the stiffness of matrix (Fig. 4.1).

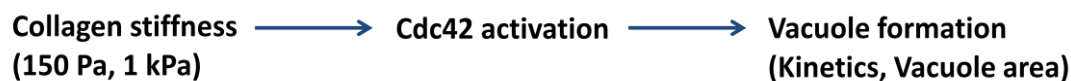


Figure 4.1 Schematic diagram illustrating the effect of collagen stiffness on Cdc42 activation and vacuole formation

Recent reports by Bailey et al. and Hanjaya-Putra et al. have described the different responses of ECFC in vacuole formation to stiffness [34, 55]. Bailey et al. have reported that increasing collagen concentration alters the stiffness of matrix and changes the vascular lumen formation of ECFCs [55]. Similarly, Hanjaya-Putra et al. have shown that vascular lumen formation was decreased in a rigid matrix, suggesting that the reduction of tension may trigger a signaling cascade which leads to vascular lumen formation [34]. Our study extends the findings of Bailey et al. and Hanjaya-Putra et al. that the stiffness of matrix alters ECFC vacuole formation in vitro.

To examine how the stiffness of matrix alters Cdc42 activity and vacuole formation, we transfected ECFCs with a FRET-based Cdc42 biosensor, and seeded them into collagen matrices with different shear storage moduli (150 Pa and 1 kPa). After hematopoietic cytokines were applied, Cdc42 was highly activated near the vacuole sites of ECFCs. In addition, Cdc42 activation preceded the vacuole formation. These results are consistent with a previous report demonstrating that Cdc42 is involved in the initiation of vacuole formation while Rac1 is involved in the enlargement and remodeling of vacuoles [44]. Moreover, Cdc42 was differentially regulated in a 3D matrix depending on its stiffness. In soft (150 Pa) matrices, Cdc42 activity steadily increased until 3 h and then started to decrease to the basal activity. However, in rigid (1 kPa) matrices, Cdc42 activity was not significantly altered during vacuole formation although its initial activation level was higher than that in soft matrices. There are several possible explanations. In rigid matrices, initial Cdc42 activity may be strong enough to induce vacuole formation. Another possible explanation is that increased matrix stiffness may activate RhoA thereby inhibiting Cdc42. Alternatively, increased collagen concentration increases collagen cross link fibril density. Thus, cytokines might diffuse slowly so that Cdc42 activation is hindered.

To investigate the kinetics of early vacuole formation, we compared the time point of early vacuole formation between soft and rigid collagen matrices. By analyzing the pattern of early vacuole formation, we observed that vacuoles formed earlier in soft matrices than rigid matrices. Most of the vacuoles were formed at 2 to 3 h in soft matrices, while they were formed at 3 to 4 h in rigid matrices. These data suggest one hour shifts of vacuole formation in rigid collagen matrices and soft matrices cause faster vacuole formation than that of rigid stiffness. Together with Cdc42 activity data, these results suggest that an increase in Cdc42 activity stimulates vacuole formation and these responses are dependent on matrix stiffness.

Next, we postulated that if matrix stiffness regulated Cdc42 activity and initiation of vacuole formation, it would alter the morphology of the vacuoles. We observed that average vacuole area was $106.1 \mu\text{m}^2$ and $100.3 \mu\text{m}^2$ in soft and rigid matrices, respectively. Although mean vacuole area in soft matrices was 6% larger than that in rigid matrices, they did not show a significant difference. There is a discrepancy in previous reports on lumen size and matrix stiffness. Increased matrix stiffness has shown to decrease endothelial lumen formation and average lumen area [34, 55]. Opposite results have also been reported that vacuole area is increased in rigid matrices [53, 54]. These reports have suggested that an increase of stiffness activates RhoA, which facilitates angiogenesis and capillary branching [90]. Also, it has been demonstrated that tumor tissues which are stiffer than normal tissues developed a large vascular lumen [53]. This discrepancy may be due to different endothelial source, matrix composition, and the measurement methods.

To further investigate the role of Cdc42 in early vacuole formation, we used two Cdc42 mutants: constitutively active Cdc42 (Cdc42-L61) and dominant negative Cdc42 (Cdc42-N19). Our results demonstrated that Cdc42-L61 promotes vacuole formation, while Cdc42-N19 inhibits it. This result is consistent with previous study using Cdc42 siRNA that Cdc42 inhibition suppressed lumen formation of ECs in 3D collagen matrices [69]. In our study, Cdc42-N17 did not completely suppress vacuole formation. This could

be due to drawbacks of using dominant mutants of Rho GTPases [91]. The principle of dominant mutant is threonine residue at 17th amino acid is changed to asparagine and the mutants binds to GEFs with high affinity to make dead-ends [92]. The result of inhibition, however, may be distorted by the expression level of the mutant and interaction with other Rho family GTPases [91].

In conclusion, we demonstrated that the stiffness of collagen matrices alters Cdc42 activity and regulates early vacuole formation of ECFCs. Local Cdc42 activation induces vacuole formation and its activity is associated with dynamics of vacuole formation. The results presented here suggest that mechanical balance between ECFCs and matrices is an important parameter to regulate vascularization. Future studies will address how Rac1 or Cdc42 interacts with matrix metalloproteinases such as MT1-MMP in response to matrix stiffness.

LIST OF REFERENCES

LIST OF REFERENCES

- [1] A. Wacker and H. Gerhardt, "Endothelial development taking shape," *Curr, Opin. Cell Biol.*, Vol. 23, No. 6, pp. 676-685, 2011.
- [2] D. Lyden, K. Hattori, S. Dias, C. Costa, P. Blaikie, L. Butros, A. Chadburn, B. Heissiq, W. Marks, L. Witte, Y. Wu, D. Hicklin, Z. Zhu, N. R. Hackett, R. G. Crystal, M. A. Moore, K. A. Haiiar, K. Manova, R. Benezra, and S. Rafii, "Impaired recruitment of bone-marrow-derived endothelial and hematopoietic precursor cells blocks tumor angiogenesis and growth," *Nat. Med.*, Vol. 7, No. 11, pp. 1194-1201, 2001.
- [3] W. Risau, "Mechanisms of angiogenesis," *Nature*, Vol. 386, No. 6626, pp. 671-674, 1997.
- [4] P. Carmeliet and R. K. Jain, "Angiogenesis in cancer and other diseases," *Nature*, Vol. 407, No. 6801, pp. 249-257, 2000.
- [5] R. K. Jain, P. Au, J. Tam, D. G. Duda, and D. Fukumura, "Engineering vascularized tissue," *Nat. Biotechnol.*, Vol. 23, No. 7, pp. 821-823, 2005.
- [6] A. Kawamoto and T. Asahara, "Role of progenitor cells in cardiovascular disease and upcoming therapies," *Catheter Cardiovasc. Interv.*, Vol. 70, No. 4, pp. 477-484, 2007.
- [7] J. Folkman and C. Haudenschild, "Angiogenesis in vitro," *Nature*, Vol. 288, No. 5791, pp. 551-556, 1980.
- [8] M. P. Lutolf and J. A. Hubbell, "Synthetic biomaterials as instructive extracellular microenvironments for morphogenetic in tissue engineering," *Nat. Biotechnol.*, Vol. 23, No. 1, pp. 47-55, 2005.
- [9] J. Folkman, P. Hahnfeltd, and L. Hlatky, "Cancer: looking outside the genome," *Nat. Rev. Mol. Cell Biol.*, Vol. 1, No. 1, pp. 76-79, 2000.

- [10] J. S. Schechner, A. K. Nath, L. Zheng, M. S. Kluger, C. C. Hughes, M. R. Sierra-Honigmann, M. I. Lorber, G. Tellides, M. Kashgarian, A. L. Bothwell, and J. S. Pober, "In vivo formation of complex microvessels lined by human endothelial cells in an immunodeficient mouse," *Proc. Natl. Acad. Sci.*, Vol. 97, No. 16, pp. 9191-9196, 2000.
- [11] N. Koike, D. Fukumura, O. Gralla, P. Au, J. S. Schechner, and R. K. Jain, "Tissue engineering: creation of long-lasting blood vessels," *Nature*, Vol. 428, No. 6979, pp. 138-139, 2004.
- [12] A. Lesman, M. Habib, O. Caspi, A. Gepstein, G. Arbel, S. Levenberg, and L. Gepstein, "Transplantation of a tissue-engineered human vascularized cardiac muscle," *Tissue Eng. Part A*, Vol. 16, No. 1, pp. 115-125, 2010.
- [13] J. M. Melero-Martin, Z. A. Khan, A. Picard, X. Wu, S. Paruchuri, and J. Bischoff, "In vivo vasculogenic potential of human blood-derived endothelial progenitor cells," *Blood*, Vol. 111, No. 3, pp. 4761-4768, 2007.
- [14] V. J. Dzau, M. Gnecci, A. S. Pachori, F. Morello, and L. G. Melo, "Therapeutic potential of endothelial progenitor cells in cardiovascular diseases," *Hypertension*, Vol. 46, No. 1, pp. 7-18, 2005.
- [15] C. Urbich and S. Dimmeler, "Endothelial progenitor cells characterization and role in vascular biology," *Circ. Res.*, Vol. 95, No. 4, pp. 343-353, 2004.
- [16] Z. M. Hill, G. Zalos, J. P. Halcox, W. H. Schenke, M. A. Waclawiw, A. A. Quyyumi, and T. Finkle, "Circulating endothelial progenitor cells, vascular function, and cardiovascular risk," *N. Engl. J. Med.*, Vol. 348, No. 7, pp. 593-600, 2003.
- [17] D. N. Prater, J. Case, D. A. Ingram, and M. C. Yoder, "Working hypothesis to redefine endothelial progenitor cells," *Leukemia*, Vol. 21, No. 6, pp. 1141-1149, 2007.
- [18] D. A. Ingram, L. E. Mead, H. Tanaka, V. Meade, A. Fenoglio, K. Mortell, K. Pollok, M. J. Ferkowicz, D. Gilley, and M. C. Yoder, "Identification of a novel hierarchy of endothelial progenitor cells using human peripheral and umbilical cord blood," *Blood*, Vol. 104, No. 9, pp. 2752-2760, 2004.
- [19] P. J. Crister, S. L. Voytik-Harbin, and M. C. Yoder. "Isolating and defining cells to engineer human blood vessels," *Cell Prolif.*, Vol. 44, Suppl. 1, pp. 15-21, 2011.
- [20] S. Sen, S. P. McDonald, P. T. Coates, and C. S. Bonder, "Endothelial progenitor cells: novel biomarker and promising cell therapy for cardiovascular disease," *Clin. Sci. (Lond.)*, Vol. 120, No. 7, pp. 263-283, 2011.

- [21] T. Asahara, T. Murohara, A. Sullivan, M. Silver, R. van der Zee, T. Li, B. Witzenbichler, G. Schatteman, and J. M. Isner, "Isolation of putative progenitor endothelial cells for angiogenesis," *Science*, Vol. 275, No. 5302, pp. 964-967, 1997.
- [22] C. Kalka, H. Masuda, T. Takahashi, W. M. Kalka-Moll, M. Silver, M. Kearney, T. Li, J. M. Isner, and T. Asahara, "Transplantation of ex vivo expanded endothelial progenitor cells for therapeutic neovascularization," *Proc. Natl. Acad. Sci.*, Vol. 97, No. 7, pp. 3422-3427, 2000.
- [23] P. J. Crister and M. C. Yoder, "Endothelial colony-forming cell role in neoangiogenesis and tissue repair," *Curr. Opin. Organ Transplant*, Vol. 15, No. 1, pp. 68-72, 2010.
- [24] M. Prokopi, G. Pula, U. Mayr, C. Devue, J. Gallagher, Q. Xiao, C. M. Boulanger, N. Westwood, C. Urbich, J. Willeit, M. Steiner, J. Breuss, Q. Xu, S. Kiechl, and M. Mayr, "Proteomic analysis reveals presence of platelet microparticles in endothelial progenitor cell cultures," *Blood*, Vol. 114, No. 3, pp. 723-732, 2009.
- [25] M. C. Yoder, L. E. Mead, D. Prater, T. R. Krier, K. N. Mroueh, F. Li, R. Krasich, C. J. Temm, J. T. Prchal, and D. A. Ingram, "Redefining endothelial progenitor cells via clonal analysis and hematopoietic stem/progenitor cell principals," *Blood*, Vol. 109, No. 5, pp. 1801-1809, 2007.
- [26] Y. Lin, D. J. Weisdorf, A. Solovey, and R. P. Heibel, "Origins of circulating endothelial cells and endothelial outgrowth from blood," *J. Clin. Invest.*, Vol. 105, No. 1, pp. 71-77, 2000.
- [27] A. N. Stratman, K. M. Malotte, R. D. Mahan, M. J. Davis, and G. E. Davis, "Pericyte recruitment during vasculogenic tube assembly stimulates endothelial basement membrane matrix formation," *Blood*, Vol. 114, No. 24, pp. 5091-5101, 2009.
- [28] G. E. Davis and D. R. Senger, "Endothelial extracellular matrix biosynthesis, remodeling, and functions during vascular morphogenesis and neovessel stabilization," *Circ. Res.*, Vol. 97, No. 11, pp. 1093-1107, 2005.
- [29] T. P. Kraehenbuehl, L. S. Ferreira, P. Zammaretti, J. A. Hubbell, and R. Langer, "Cell-responsive hydrogel for encapsulation of vascular cells," *Biomaterials*, Vol. 30, No. 26, pp. 4318-4324, 2009.
- [30] A. Lesman, J. Koffler, R. Atlas, Y. J. Blinder, Z. Kam, and S. Levenberg, "Engineering vessel-like networks within multicellular fibrin-based constructs," *Biomaterials*, Vol. 32, No. 31, pp. 7856-7869, 2011.

- [31] J. L. Drury and D. J. Mooney, "Hydrogel for tissue engineering: scaffold design variables and applications," *Biomaterials*, Vol. 24, No. 24, pp. 4337-4351, 2003.
- [32] H. J. Sung, C. Meredith, C. Johnson, and Z. S. Galis, "The effect of scaffold degradation rate of three-dimensional cell growth and angiogenesis," *Biomaterials*, Vol. 25, No. 26, pp. 5735-5742, 2004.
- [33] J. A. Pedersen and M. A. Swartz, "Mechanobiology in the third dimension," *Ann. Biomed. Eng.*, Vol. 33, No. 11, pp. 1469-1490, 2005.
- [34] D. Hanjaya-Putra, J. Yee, D. Ceci, R. Truitt, D. Yee, and S. Gerecht, "Vascular endothelial growth factor and substrate mechanics regulate in vitro tubulogenesis of endothelial progenitor cells," *J. Cell. Mol. Med.* Vol. 14, No. 10, pp. 2436-2447, 2010.
- [35] E. A. Silva, E. S. Kim, H. J. Kong, and D. J. Mooney, "Material-based deployment enhances efficacy of endothelial progenitor cells," *Proc. Natl. Acad. Sci.*, Vol. 105, No. 38, pp. 14347-14352, 2008.
- [36] E. Luong and S. Gerecht, "Stem cells and scaffolds for vascularizing engineered tissue constructs," *Adv. Biochem. Eng. Biotechnol.*, Vol. 114, pp. 129-172, 2009.
- [37] H. K. Kleinman and G. R. Martin, "Matrigel: basement membrane matrix with biological activity," *Semin. Cancer Biol.*, Vol. 15, No. 5, pp. 378-386, 2005.
- [38] T. Twardowski, A. Fertala, J. P. Orgel, and J. D. San Antonio, "Type I collagen and collagen mimetics as angiogenesis promoting superpolymers," *Curr. Pharm. Des.*, Vol. 13, No. 35, pp. 3608-3621, 2007.
- [39] S. T. Kreger, B. J. Bell, J. Bailey, E. Stites, J. Kuske, B. Waisner, and S. L. Voytik-Harbin, "Polymerization and matrix physical properties as important design consideration for soluble collagen formulations," *Biopolymers*, Vol. 93, No. 8, pp. 690-707, 2010.
- [40] C. P. Blobel, "3D trumps 2D when studying endothelial cells," *Blood*, Vol. 115, No. 25, pp. 5128-5130, 2010.
- [41] S. Fernandez-Sauze, D. Grall, B. Cseh, and E. Van Obberghen-Schilling, "Regulation of fibronectin matrix assembly and capillary morphogenesis in endothelial cells by Rho family GTPases," *Exp. Cell Res.*, Vol. 315, No. 12, pp. 2092-2104, 2009.
- [42] A. Stèphanou, G. Meskaoui, B. Vailhè, and P. Tracqui, "The rigidity in fibrin gels as a contributing factor to the dynamics of *in vitro* vascular cord formation," *Miscrovasc. Res.*, Vol. 73, No. 3, pp. 182-190, 2007.

- [43] G. E. Davis and C. W. Camarillo, "An $\alpha 2\beta 1$ integrin-dependent pinocytic mechanism involving intracellular vacuole formation and coalescence regulates capillary lumen and tube formation in three-dimensional collagen matrix," *Exp. Cell Res.*, Vol. 224, No. 1, pp. 39-51, 1996.
- [44] K. J. Bayless and G. E. Davis, "The Cdc42 and Rac1 GTPases are required for capillary lumen formation in three-dimensional extracellular matrices," *J. Cell Sci.*, Vol. 115, Pt. 6, pp. 1123-1136, 2002.
- [45] N. Wang, J. P. Butler, and D. E. Ingber, "Mechanotransduction across the cell surface and through the cytoskeleton," *Science*, Vol. 260, No. 5111, pp. 1124-1127, 1993.
- [46] M. A. Wozniak, K. Modzelewska, L. Kwong, and P. J. Keely, "Focal adhesion regulation of cell behavior," *Biochem. Biophys. Acta.*, Vol. 1692, No. 2-3, pp. 103-119, 2004.
- [47] S. A. Ruiz and C. S. Chen, "Emergence of patterned stem cell differentiation within multicellular structures," *Stem Cells*, Vol. 26, No. 11, pp. 2921-2927, 2008.
- [48] A. J. Engler, S. Sen, H. L. Sweeney, and D. E. Discher, "Matrix elasticity directs stem cells lineage specification," *Cell*, Vol. 126, No. 4, pp. 667-689, 2006.
- [49] K. Saha, A. J. Keung, E. F. Irwin, Y. Li, L. Little, D. V. Schaffer, and K. E. Healy, "Substrate modulus directs neural stem cell behavior," *Biophys. J.*, Vol. 95, No. 9, pp. 4426-4438, 2008.
- [50] J. P. Califano and C. A. Reinhart-King, "A balance of substrate mechanics and matrix chemistry regulates endothelial cell network assembly," *Cellular and Molecular Bioengineering*, Vol. 1, No. 2-3, pp. 122-132, 2008.
- [51] C. M. Ghajar, X. Chen, J. W. Harris, V. Suresh, C. C. Hughes, N. L. Jeon, A. J. Putnam, and S. C. George, "The effect of matrix density on the regulation of 3-D capillary morphogenesis," *Biophys. J.*, Vol. 94, No. 5, pp. 1930-1941, 2008.
- [52] E. Kniazeva and A. J. Andrew, "Endothelial cell traction and ECM density influence both capillary morphogenesis and maintenance in 3-D," *Am. J. Physiol. Cell Physiol.*, Vol. 297, No. 1, pp. 179-187, 2009.
- [53] A. L. Sieminski, R. P. Hebbel, and K. J. Gooch, "The relative magnitudes of endothelial force generation and matrix stiffness modulate capillary morphogenesis in vitro," *Exp. Cell Res.*, Vol. 297, No. 2, pp. 574-584, 2004.

- [54] N. Yamamura, R. Sudo, M. Ikeda, and K. Tanishita, "Effects of the mechanical properties of collagen gel on the *in vitro* formation of microvessel network by endothelial cells," *Tissue Eng.*, Vol. 13, No. 7, pp. 1443-1453, 2007.
- [55] J. L. Bailey, P. J. Crister, C. Whittington, J. L. Kuske, M. C. Yoder, S. L. Voytik-Harbin, "Collagen oligomers modulate physical and biological properties of three-dimensional self-assemble matrices," *Biopolymers*, Vol. 95, No. 2, pp. 77-93, 2011.
- [56] P. J. Crister, S. T. Kreger, S. L. Voytik-Harbin, M. C. Yoder, "Collagen matrix physical properties modulate endothelial colony forming cell-derived vessels *in vivo*." *Microvasc. Res.*, Vol. 80, No. 1, pp. 23-30, 2010.
- [57] G. T. Meyer, L. J. Matthias, L. Noack, M. A. Vadas, and J. R. Gamble, "Lumen formation during angiogenesis *in vitro* involves phagocytic activity, formation and secretion of vacuoles, cell death, and capillary tube remodeling by different populations of endothelial cells," *Anat. Rec.*, Vol. 249, No. 3, pp. 327-340, 1997.
- [58] M. Kamei, W. B. Saunders, K. J. Bayless, L. Dye, G. E. Davis, and B. M. Weinstein, "Endothelial tubes assemble from intracellular vacuoles *in vivo*," *Nature*, Vol. 442, No. 7101, pp. 453-456, 2006.
- [59] G. E. Davis, W. Koh, and A. N. Stratman, "Mechanisms controlling human endothelial lumen formation and tube assembly in three-dimensional extracellular matrices," *Birth Defects Res. C Embryo Today*, Vol. 81, No. 4, pp. 270-285, 2007.
- [60] A. C. Zovein, A. Luque, K. A. Turlo, J. J. Hofmann, K. M. Yee, M. S. Becker, R. Fassler, I. Mellman, T. F. Lane, and M. L. Iruela-Arispe, " β 1 integrin establishes endothelial cell polarity and arteriolar lumen formation via a Par3-dependent mechanism," *Dev. Cell*, Vol. 18, No. 1, pp. 39-51, 2010.
- [61] Y. Liu, Y. Li, and Y. Xu, "Inhibitory effects of novel integrin-targeting peptides on angiogenesis activity in HUVEC cell *in vitro*," *Cell Biochem. Funct.*, Vol. 29, No. 5, pp. 429-435, 2011.
- [62] R. O. Hynes, "Cell-matrix adhesion in vascular development," *J. Thromb. Haemost.*, Vol. 5, Suppl. 1, pp. 32-40, 2007.
- [63] J. R. Gamble, L. J. Matthias, G. Meyer, P. Kaur, G. Russ, R. Faull, M. C. Berndt, and M. A. Vadas, "Regulation of *in vitro* capillary tube formation by anti-integrin antibodies," *J. Cell Biol.*, Vol. 121, No. 4, pp. 931-943, 1993.
- [64] A. Hall, "Rho GTPases and the actin cytoskeleton," *Science*, Vol. 279, No. 5350, pp. 509-514, 1998.

- [65] S. Etienne-Manneville and A. Hall, "Rho GTPases in cell biology," *Nature*, Vol. 420, No. 6916, pp. 629-635, 2002.
- [66] N. S. Sipes, Y. Feng, F. Guo, H. O. Lee, F. S. Chou, J. Cheng, J. Mulloy, and Y. Zheng, "Cdc42 regulates extracellular matrix remodeling in three dimensions," *J. Biol. Chem.*, Vol. 286, No. 42, pp. 36469-36477, 2011.
- [67] N. Lakshman, A. Kim, K. J. Bayless, G. E. Davis, and W. M. Petroll, "Rho plays a central role in regulating local cell-matrix mechanical interactions in 3D culture," *Cell Motil. Cytoskeleton*, Vol. 64, No. 6, pp. 434-445, 2007.
- [68] T. M. Seasholtz and J. H. Brown, "Rho signaling in vascular diseases," *Mol. Interv.*, Vol. 4, No. 6, pp. 348-357, 2004.
- [69] W. Koh, R. D. Mahan, G. E. Davis, "Cdc42- and Rac1-mediated endothelial lumen formation requires Pak2, Pak4 and Par3, and PKC-dependent signaling," *J. Cell Sci.*, Vol. 121, Pt. 7, pp. 989-1001, 2008.
- [70] W. Koh, K. Sachidanandam, A. N. Stratman, A. Sacharidou, A. M. Mayo, E. A. Murphy, D. A. Cheresh, and G. E. Davis, "Formation of endothelial lumens requires a coordinated PKC ϵ -, Src-, Pak- and Raf-kinase-dependent signaling cascade downstream of Cdc42 activation," *J. Cell Sci.*, Vol. 122, Pt. 11, pp. 1812-1822, 2009.
- [71] A. Sacharidou, W. Koh, A. N. Stratman, A. M. Mayo, K. E. Fisher, and G. E. Davis, "Endothelial lumen signaling complexes control 3D matrix-specific tubulogenesis through interdependent Cdc42- and MT1-MMP-mediated events," *Blood*, Vol. 115, No. 25, pp. 5259-5269, 2010.
- [72] B. Strilić, T. Kućera, J. Eqlinger, M. R. Hughes, K. M. McNagny, S. Tsukita, E. Dejana, N. Ferrara, and E. Lammert, "The molecular basis of vascular lumen formation in the developing mouse aorta," *Dev. Cell*, Vol. 17, No. 4, pp. 505-515, 2009.
- [73] K. J. Whitehead, A. C. Chan, S. Navankasattusas, W. Koh, N. R. London, J. Ling, A. H. Mayo, S. G. Drakos, C. A. Jones, W. Zhu, D. A. Marchuk, G. E. Davis, and D. Y. Li, "The cerebral cavernous malformation signaling pathway promotes vascular integrity via Rho GTPases," *Nat. Med.*, Vol. 15, No. 2, pp. 177-184, 2009.
- [74] K. Xu, A. Sacharidou, S. Fu, D. C. Chong, B. Skaug, Z. J. Chen, G. E. Davis, and O. Cleaver, "Blood vessel tubulogenesis requires Rasip1 regulation of GTPase signaling," *Dev. Cell*, Vol. 20, No. 4, pp. 526-539, 2011.

- [75] E. Ellertsdóttir, A. Lenard, Y. Blum, A. Krudewig, L. Herwig, M. Affolter, and H. G. Belting, "Vascular morphogenesis in the zebrafish embryo." *Dev. Biol.*, Vol. 341, No. 1, pp. 56-65, 2010.
- [76] M. V. Hoang, J. A. Nagy, and D. R. Senger, "Cdc42-mediated inhibition of GSK-3 β improves angio-architecture and lumen formation during VEGF-driven pathological angiogenesis," *Microvasc. Res.*, Vol. 81, No. 1, pp. 34-43, 2011.
- [77] M. Zeeb, B. Strlic, and E. Lammert, "Resolving cell-cell junctions: lumen formation in blood vessels," *Curr. Opin. Cell Biol.*, Vol. 22, No. 5, pp. 626-632, 2010.
- [78] D. M. Chudakov, M. V. Matz, S. Lukyanov, and K. A. Lukyanov, "Fluorescent proteins and their applications in imaging living cells and tissues," *Physiol. Rev.*, Vol. 90, No. 3, pp. 1103-1163, 2010.
- [79] T. Nakamura, K. Aoki, and M. Matsuda, "Monitoring spatio-temporal regulation of Ras and Rho GTPases with GFP-based FRET probes," *Methods*, Vol. 37, No. 2, pp. 146-153, 2005.
- [80] R. E. Itoh, K. Kurokawa, Y. Ohba, H. Yoshizaki, M. Mochizuki, and M. Matsuda, "Activation of Rac and Cdc42 video imaged by fluorescent resonance energy transfer-based singly-molecule probes in the membrane of living cells," *Mol. Cell Biol.*, Vol. 22, No. 18, pp. 6582-6591, 2002.
- [81] H. Yoshizaki, Y. Ohba, K. Kurokawa, R. E. Itoh, T. Nakamura, N. Mochizuki, K. Nagashima, and M. Matsuda, "Activity of Rho-family GTPases during cell division as visualized with FRET-based probes," *J. Cell Biol.*, Vol. 162, No. 2, pp. 223-232, 2003.
- [82] T. Yokono, H. Kotaniguchi, and Y. Fukui, "Clear imaging of Förster resonance transfer (FRET) signals of Ras activation by a time-lapse three-dimensional deconvolution system," *J. Microsc.*, Vol. 223, Pt. 1, pp. 9-14, 2006.
- [83] A. N. Stratman, M. J. Davis, and G. E. Davis, "VEGF and FGF prime vascular tube morphogenesis and sprouting directly by hematopoietic stem cell cytokines," *Blood*, Vol. 117, No. 14, pp. 3709-3719, 2011.
- [84] W. Koh, A. N. Stratman, A. Sacharidou, and G. E. Davis, "In vitro three dimensional collagen matrix models of endothelial lumen formation during vasculogenesis and angiogenesis," *Methods Enzymol.*, Vol. 443, pp. 83-101, 2008.
- [85] E. Kardash, J. Bandemer, and E. Raz, "Imaging protein activity in live embryos using fluorescence resonance energy transfer biosensors," *Nature Protocol*, Vol. 6, No. 12, pp. 1835-1846, 2011.

- [86] O. Pertz, L. Hodgson, R. L. Klemke, and K. M. Hahn, "Spatiotemporal dynamics of RhoA activity in migrating cells," *Nature*, Vol. 440, No. 7087, pp. 1069-1072, 2006.
- [87] M. Machacek, L. Hodgson, C. Welch, H. Elliott, O. Pertz, P. Nalbant, A. Abell, G. L. Johnson, K. M. Hahn, and G. Danuser, "Coordination of Rho GTPase activities during cell protrusion," *Nature*, Vol. 461, No. 7260, pp. 99-103, 2009.
- [88] K. Kurokawa, T. Nakamura, K. Aoki, and M. Matsuda, "Mechanism and role of localized activation of Rho-family GTPase in growth factor-stimulated fibroblasts and neuronal cells," *Biochem. Soc. Trans.*, Vol. 33, Pt. 4, pp. 631-634, 2005.
- [89] B. Liu, T. J. Kim, and Y. Wang, "Live cell imaging of mechanotransduction," *J. R. Soc. Interface*, Vol. 7, Suppl. 3, pp. S365-S375, 2010.
- [90] A. Mammoto, T. Mammoto, D. E. Ingber, "Rho signaling and mechanical control of vascular development," *Curr. Opin. Hematol.*, Vol. 15, No. 3, pp. 228-234, 2008.
- [91] A. Czuchra, X. Wu, H. Meyer, J. van Hengel, T. Schroeder, R. Geffers, K. Rottner, and C. Brakebusch, "Cdc42 is not essential for filopodium formation, directed migration, cell polarization, cell polarization, and mitosis in fibroblastoid cells," *Mol. Biol. Cell*, Vol. 16, No. 10, pp. 4473-4484, 2005.
- [92] L. A. Feig, "Tools of the trade: use of dominant-inhibitory mutants of Ras-family GTPases," *Nat. Cell Biol.*, Vol. 1, No. 2, pp. E25-E27, 1999.